with infusional 5FU, may be an attractive arm for a Phase III trial in CRC, with CPT-11/5FU as the control arm. We have already initiated a Phase I trial of NK012 in patients with advanced solid tumors based on the data suggesting higher efficacy and lower toxicity of this preparation than CPT-11 *in vivo*.[12]

In conclusion, we demonstrated that combined NK012 and 5FU chemotherapy exerts significantly greater antitumor activity against human CRC xenografts as compared to CPT-11/5FU, indicating the necessity of clinical evaluation of this combined regimen.

References

1. Saltz LB, Douillard JY, Pirotta N, Alakl M, Gruia G, Awad L, Elfring GL, Locker PK, Miller LL. Irinotecan plus fluorouracil/leucovorin for metastatic colorectal cancer: a new survival standard. Oncologist 2001;6:81–91.
2. Douillard JY, Cunningham D, Roth AD, Navarro M, James RD, Karasek P, Jandik P, Iveson T, Carmichael J, Alakl M, Gruia G, Awad L, et al. Irinotecan combined with fluorouracil compared with fluorouracil alone as first-line treatment for metastatic colorectal cancer: a multicentre randomised trial. Lancet 2000;355:1041–7.
3. Takimoto CH, Arbuck SG. Topoisomerase I targeting agents: the camptothecins. In: Chabner BA, Lango DL, eds. Cancer chemotherapy and biotherapy: principal and practice, 3rd ed. Philadelphia, PA: Lippincott Williams and Wilkins, 2001. 579–646.
4. Slatter JG, Schaaf LJ, Sams JP, Feenstra KL, Johnson MG, Bombardt PA, Cathcart KS, Verburg MT, Pearson LK, Compton LD, Miller LL, Baker DS, et al. Pharmacokinetics, metabolism, and excretion of irinotecan (CPT-11) following I.V. infusion of [(14)C]CPT-11 in cancer patients. Drug Metab Dispos 2000;28:423–33.
5. Rothenberg ML, Kuhn JG, Burris HA, III, Nelson J, Eckardt JR, Tristan-Morales M, Hilsenbeck SG, Weiss GR, Smith LS, Rodriguez GI, Rock MK, Von Hoff DD. Phase I and pharmacokinetic trial of weekly CPT-11. J Clin Oncol 1993;11:2194–204.
6. Guichard S, Terret C, Hennebelle I, Lochon I, Chevreau P, Fretigny E, Selves J, Chatelut E, Bugat R, Canal P. CPT-11 converting carboxylesterase and topoisomerase activities in tumour and normal colon and liver tissues. Br J Cancer 1999;80:364–70.
7. Gradishar WJ, Tjulandin S, Davidson N, Shaw H, Desai N, Bhar P, Hawkins M, O'Shaughnessy J. Phase III trial of nanoparticle albumin-bound paclitaxel compared with polyethylated castor oil-based paclitaxel in women with breast cancer. J Clin Oncol 2005;23:7794–803.
8. Muggia FM. Liposomal encapsulated anthracyclines: new therapeutic horizons. Curr Oncol Rep 2001;3:156–62.
9. Matsumura Y, Maeda H. A new concept for macromolecular therapeutics in cancer chemotherapy: mechanism of tumoritropic accumulation of proteins and the antitumor agent smancs. Cancer Res 1986;46:6387–92.
10. Zhang JA, Xuan T, Parmar M, Ma L, Ugwu S, Ali S, Ahmad I. Development and characterization of a novel liposome-based formulation of SN-38. Int J Pharm 2004;270:93–107.
11. Kraut EH, Fishman MN, LoRusso PM, Gorden MS, Rubin EH, Haas A, Fetterly GJ, Cullinan P, Dul JL, Steinberg JL. Final result of a phase I study of liposome encapsulated SN-38 (LE-SN38): safety, pharmacogenomics, pharmacokinetics, and tumor response [abstract 2017]. Proc Am Soc Clin Oncol 2005;23:139S.
12. Koizumi F, Kitagawa M, Negishi T, Onda T, Matsumoto S, Hamaguchi T, Matsumura Y. Novel SN-38-incorporating polymeric micelles. NK012, eradicate vascular endothelial growth factor-secreting bulky tumors. Cancer Res 2006;66:10048–56.
13. Chou TC, Talalay P. Quantitative analysis of dose-effect relationships: the combined effects of multiple drugs or enzyme inhibitors. Adv Enzyme Regul 1984;22:27–55.
14. Azrak RG, Cao S, Slocum HK, Toth K, Durrani FA, Yin MB, Pendyala L, Zhang W, McLeod HL, Rustum YM. Therapeutic synergy between irinotecan and 5-fluorouracil against human tumor xenografts. Clin Cancer Res 2004;10:1121–9.
15. Jain RK. Barriers to drug delivery in solid tumors. Sci Am 1994; 271:58–65.
16. Savic R, Luo L, Eisenberg A, Maysinger D. Micellar nanocontainers distribute to defined cytoplasmic organelles. Science 2003;300:615–18.
17. Kawato Y, Aonuma M, Hirota Y, Kuga H, Sato K. Intracellular roles of SN-38, a metabolite of the camptothecin derivative CPT-11, in the antitumor effect of CPT-11. Cancer Res 1991;51:4187–91.
18. Slater R, Radstone D, Matthews L, McDaid J, Majeed A. Hepatic resection for colorectal liver metastasis after downstaging with irinotecan improves survival. Proc Am Soc Clin Oncol 2003;22(abstract 1287).
19. Araki E, Ishikawa M, Iigo M, Koide T, Itabashi M, Hoshi A. Relationship between development of diarrhea and the concentration of SN-38, an active metabolite of CPT-11, in the intestine and the blood plasma of athymic mice following intraperitoneal administration of CPT-11. Jpn J Cancer Res 1993;84:697–702.
20. Atsumi R, Suzuki W, Hakusui H. Identification of the metabolites of irinotecan, a new derivative of camptothecin, in rat bile and its biliary excretion. Xenobiotica 1991;21:1159–69.
21. Onda T, Nakamura I, Seno C, Matsumoto S, Kitagawa M, Okamoto K, Nishikawa K, Suzuki M. Superior antitumor activity of NK012, 7-ethyl-10-hydroxycamptoyhecin-incorporating micellar nanoparticle, to irrinotecan. Proc Am Assoc Cancer Res 2006;47:720s(abstract 3062).
22. Tournigand C, Andre T, Achille E, Lledo G, Flesh M, Mery-Mignard D, Quinaux E, Couteau C, Buyse M, Ganem G, Landi B, Colin P, et al. FOLFIRI followed by FOLFOX6 or the reverse sequence in advanced colorectal cancer: a randomized GERCOR study. J Clin Oncol 2004;22:229–37.
23. Colucci G, Gebbia V, Paoletti G, Giuliani F, Caruso M, Gebbia N, Carteni G, Agostara B, Pezzella G, Manzione L, Borsellino N, Misino A, et al. Phase III randomized trial of FOLFIRI versus FOLFOX4 in the treatment of advanced colorectal cancer: a multicenter study of the Gruppo Oncologico Dell'Italia Meridionale. J Clin Oncol 2005; 23:4866–75.

Thioredoxin2 enhances the damaged DNA binding activity of mtTFA through direct interaction

AKIHIKO KIDANI[1,2], HIROTO IZUMI[1], YOICHIRO YOSHIDA[3], EIJI KASHIWAGI[1], HARUKI OHMORI[2], TSUNEO TANAKA[2], MICHIHIKO KUWANO[4] and KIMITOSHI KOHNO[1]

[1]Department of Molecular Biology, School of Medicine, University of Occupational and Environmental Health, Kitakyushu; [2]Department of Digestive and General Surgery, Faculty of Medicine, Shimane University, Izumo; [3]Osaka Rosai Hospital, Surgery, Sakai; [4]Innovative Anticancer Diagnosis and Therapeutics, Innovation Center for Medical Redox Navigation, Kyushu University, Fukuoka, Japan

Received July 22, 2009; Accepted September 16, 2009

DOI: 10.3892/ijo_00000462

Abstract. Mitochondrial transcription factor A (mtTFA) is a member of the HMG (high mobility group)-box protein family. We previously showed that mtTFA preferentially binds to both cisplatin-damaged and oxidatively damaged DNA. In this study, we found that expression levels of both mtTFA and the mitochondrial antioxidant protein thioredoxin2 (TRX2) are upregulated in cisplatin-resistant cell lines. In addition, TRX2 directly interacts with mtTFA and enhances its damaged DNA binding activity. The interaction between mtTFA and TRX2 requires the HMG box 1 motif of mtTFA. Furthermore, when amino acid substitutions were introduced at either C49G or C246stop, TRX2 interacted with mtTFA. However, the interaction of TRX2 with mtTFA was enhanced when both mutations (C49G and C246stop) were introduced. Binding to cisplatin-damaged DNA was similar among mutant mtTFA proteins. By contrast, binding to oxidized DNA was significantly enhanced when double mutations were introduced. These results suggest that TRX2 not only functions as an antioxidant, but also supports mtTFA functions.

Introduction

The cytotoxic action of cisplatin is believed to result from the formation of covalent adducts with DNA. We have previously reported that cisplatin-targeted sequences, such as G-stretch sequences, are more numerous in humans and gorillas than in rodents, frogs and flies (1). Furthermore, G-stretch sequences appear much more frequently in mtDNA than in nuclear DNA. Thus, we propose that mtDNA might be the main target of cisplatin.

Reactive oxygen species (ROS) have been implicated in various pathologies (2-11). mtDNA is more susceptible to oxidative damage than genomic DNA because of its lack of a nucleosome structure. mtTFA is a member of the HMG-box protein family (12), members of which stimulate transcription by binding to the D-loop region of mtDNA and function in mtDNA maintenance and repair (13,14). Nuclear HMG-box proteins bind preferentially to cisplatin-damaged DNA (15-18). We have previously shown that mtTFA also preferentially recognizes oxidatively damaged DNA as well as cisplatin-damaged DNA (19). The enhanced binding affinity of mtTFA for damaged DNA may suggest that mtTFA protects mtDNA from various DNA damage. Additionally, mtTFA plays an important role in apoptosis. In the present study, we found that the expression levels of both mtTFA and TRX2 are upregulated in cisplatin-resistant cells. We also investigated the physical and functional interaction between mtTFA and TRX2. We found that TRX2 directly interacts with mtTFA. Our findings suggest that TRX2 not only functions as an antioxidant defense, but also cooperatively acts to support mtTFA functions.

Correspondence to: Dr Kimitoshi Kohno, Department of Molecular Biology, School of Medicine, University of Occupational and Environmental Health, 1-1 Iseigaoka, Yahatanishi-ku, Kitakyushu 807-8555, Japan
E-mail: k-kohno@med.uoeh-u.ac.jp

Abbreviations: HMG, high mobility group; mtDNA, mitochondrial DNA; PCR, polymerase chain reaction; GST, glutathione S-transferase; EDTA, ethylenediaminetetraacetic acid; DTT, dithiothreitol; PMSF, phenylmethylsulfonyl fluoride; SDS, sodium dodecyl sulfate; PBS, phosphate-buffered saline

Key words: mitochondrial transcription factor A, thioredoxin2, DNA damage

Materials and methods

Cell culture. Human epithelial cancer HeLa cells were cultured in Eagle's minimal essential medium containing 8% fetal bovine serum, which was purchased from Nissui Seiyaku (Tokyo, Japan). Cisplatin-resistant HeLa/CP4 cells were derived from HeLa cells as described previously (20) and were found to be 23 to 63-fold more resistant to cisplatin than their parental cells (21). Cell lines were maintained in a 5% CO_2 atmosphere at 37°C.

Antibodies. Anti-mtTFA was prepared as previously described (22). Anti-TRX2 (HPA000994) antibody, anti-Flag (M2)

antibody, anti-Flag (M2) affinity gel and anti-ß-actin (AC-15) antibody were purchased from Sigma (St Louis, MO, USA). Anti-HA-peroxidase (3F10) was purchased from Roche Molecular Biochemicals (Mannheim, Germany).

Plasmid construction. To obtain the full-length complementary DNA (cDNA) for human TRX2, PCR was carried out on a SuperScript cDNA library (Invitrogen, San Diego, CA) using the following primer pair: 5'-GGATCCATGGCTCAGCG ACTTCTTCTGAG-3' and 5'-TCAGCCAATCAGCTTCTT CAGGAAGG-3'. Underlines indicate the start and stop codons. The PCR product was cloned into the pGEM-T easy vector (Promega, Madison, WI). To construct Flag-tagged TRX2 expression plasmid in bacteria, the *EcoRI* fragment of TRX2 cDNA was ligated into the TH-Flag vector (23). For construction of pcDNA3-Flag-TRX2, N-terminal Flag-tagged TRX2 cDNAs were ligated into a pcDNA3 vector (Invitrogen, San Diego, CA). The construction of GST-mtTFA, GST-mtTFAΔ1.2, GST-mtTFAΔ2, and GST-mtTFAΔ1 has been described previously (19). GST-mtTFA-CC (wild-type), -GC (cysteine 49 to glycine), -CX (cysteine 246 to stop codon), and -GX (cysteine 49 to glycine and cysteine 246 to stop codon) were obtained by PCR using the following primer pairs: CC, 5'-TGGCAAGTTGTCCAAAGAAACC-3' and 5'-TTTTAACACTCCTCAGCACC-3'; GC, 5'-TGGCA AGTGGTCCAAAGAAACC-3' and 5'-TTTTAACACTCCT CAGCACC-3'; CX, 5'-TGGCAAGTTGTCCAAAGAAAC-3' and 5'-TTTTATCACTCCTCAGCACC-3'; GX, 5'-TGGCA AGTGGTCCAAAGAAACC-3' and 5'-TTTTATCACTCC TCAGCACC-3'.

Expression and purification of GST-fusion proteins. Expression and purification of GST-fusion proteins were performed as described previously (19). Briefly, GST fusion proteins induced by 1 mM isopropyl-ß-D-thiogalacto-pyranoside (Boehringer Mannheim, Mannheim, Germany) were sonicated in binding buffer (50 mM Tris-HCl pH 8.0, 1 mM EDTA, 120 mM NaCl, 10% glycerol, 0.5% Nonidet P-40, 1 mM DTT, and 0.5 mM PMSF), and soluble fractions were mixed with glutathione-Sepharose 4B (GE Healthcare Bio-Science). GST-fusion proteins eluted with 50 mM Tris-HCl (pH 8.0) and 20 mM reduced glutathione according to the manufacturer's protocol (Pharmacia, Uppsala, Sweden) were separated in SDS 10% polyacrylamide slab gels. Gel strips containing the fractionated proteins were cut and homogenized in elution-renaturation buffer (1% Triton X-100, 20 mM HEPES pH 7.6, 1 mM EDTA, 100 mM NaCl, 2 mM DTT, 0.1 mM PMSF). The eluted proteins were dialyzed in dialysis buffer (50 mM Tris-HCl pH 7.5) using a PlusOne Mini Dialysis kit (Amersham Biosciences, Piscataway, NJ).

Co-immunoprecipitation assay. Transient transfection and immunoprecipitation assays were performed as described previously (23,24). Briefly, $2x10^5$ HeLa cells were seeded into 35-mm tissue culture plates. The following day, cells were transfected with 1 μg of each of HA- and Flag-fused expression plasmids using SuperFect reagent (Qiagen, Hilden, Germany) according to the manufacturer's instructions. At 6 h post-transfection, the cells were washed with PBS, cultured at 37°C for 48 h in fresh medium and then lysed in buffer X containing 50 mM Tris-HCl (pH 8.0), 1 mM EDTA, 120 mM NaCl, 0.5% (v/v) Nonidet P-40 (NP-40), 10% (v/v) glycerol, 1 mM PMSF, and 1 mM DTT. The lysates were centrifuged at 21,000 x g for 10 min at 4°C and supernatants (300 μg) were incubated for 2 h at 4°C with anti-Flag (M2) affinity gel. Immunoprecipitated samples were washed three times with buffer X and subjected to subsequent Western blot analysis.

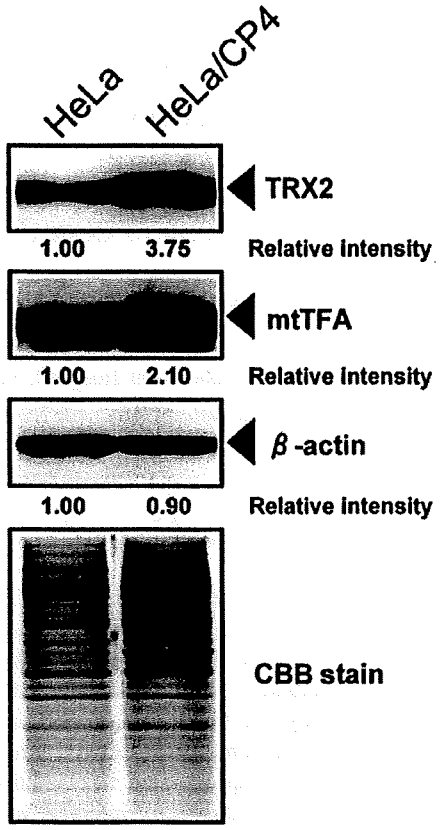

Figure 1. mtTFA and TRX2 are up-regulated in cisplatin-resistant cells. Whole-cell extracts (50 μg for mtTFA and 20 μg for TRX2) were subjected to SDS-PAGE, and Western blot analysis was done with antibodies against mtTFA, TRX2 and ß-actin (loading control). Relative intensity is shown under each blot. Gel staining with Coomassie brilliant blue (CBB) is also shown.

GST pull-down assay. Expression of TH-Flag-TRX2 and serial deletion mutants of GST-mtTFA in bacteria and GST pull-down assays were carried out as described previously (25). GST-mtTFA or its deletion mutants immobilized on glutathione-sepharose 4B were incubated with soluble bacterial extracts containing Flag-TRX2 for 2 h at 4°C in buffer X. Bound samples were washed three times with buffer X and subjected to Western blot analysis with anti-Flag antibody.

Western blot analysis. Whole-cell lysates and nuclear extracts were prepared as described previously (23,26). The indicated amounts of whole-cell lysates and nuclear extracts or immuno-precipitated samples were separated by SDS-polyacrylamide gel electrophoresis (PAGE) and transferred to polyvinylidene difluoride microporous membranes (Millipore, Bedford, MA, USA) using a semidry blotter. Blotted membranes were treated with 3% (w/v) skimmed milk in 10 mM Tris, 150 mM NaCl

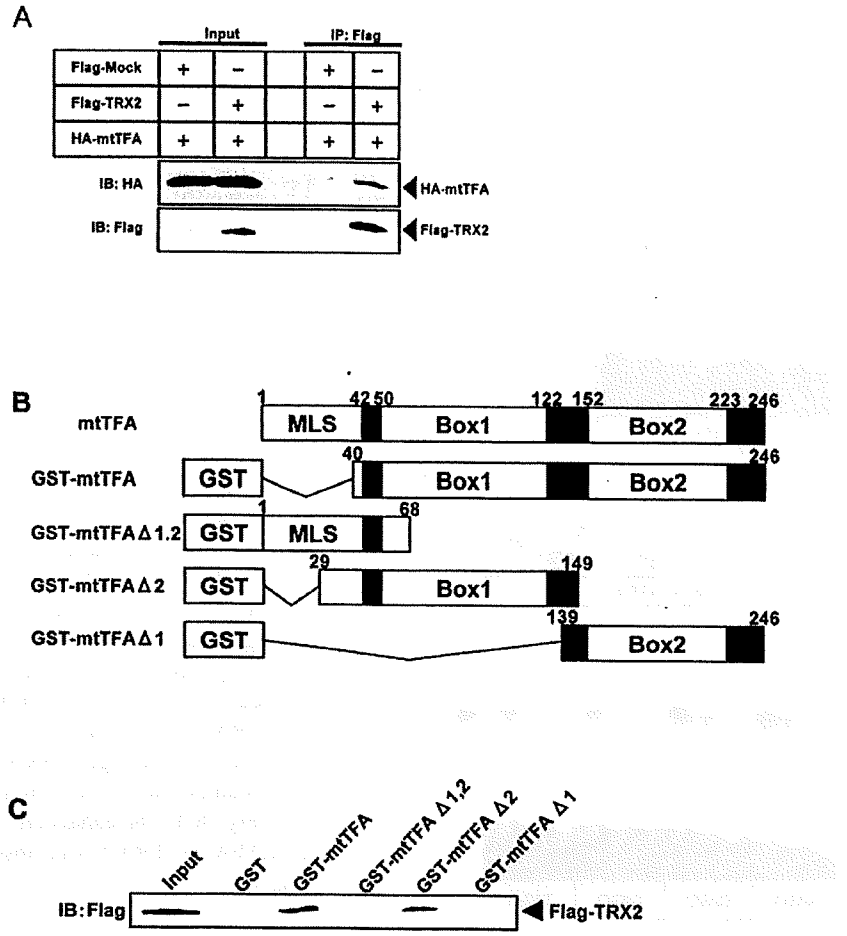

Figure 2. TRX2 directly interacts with the HMG-box 1 motif of mtTFA. (A) Whole-cell extracts (300 μg) prepared from HeLa cells co-transfected with indicated expression plasmids were immunoprecipitated with anti-Flag (M2) antibody. The resulting immunocomplexes and whole-cell extracts (30 μg) were subjected to SDS-PAGE, and Western blot analysis was performed using anti-HA and anti-Flag (M2) antibodies. (B) Schematic representation of GST-mtTFA fusion protein and the deletion mutants used in this assay. The two HMG-boxes are indicated as Box 1 and Box 2. MLS indicates mitochondrial localizing sequences. (C) GST fusion proteins immobilized on glutathione-sepharose 4B beads were incubated with Flag-TRX2 expressed in bacteria. Bound protein samples representing 10% of the input were subjected to SDS-PAGE and Western blot analysis with an anti-Flag antibody.

and 0.2% (v/v) Tween-20, and incubated for 2 h at room temperature with primary antibody. The following antibodies and dilutions were used: a 1:1000 dilution of anti-mtTFA (22), a 1:1000 dilution of anti-TRX2, a 1:10,000 dilution of anti-ß-actin, and a 1:7500 dilution of anti-Flag (M2). Membranes were then incubated for 45 min at room temperature with a peroxidase-conjugated secondary antibody or a 1:5000 dilution of anti-HA-peroxidase. Bound antibody was visualized using an enhanced chemiluminescence kit (GE Healthcare Biosciences, Piscataway, NJ, USA) and membranes were exposed to Kodak X-OMAT film (Kodak, Paris, France). For the correlation assay the intensity of each signal was quantified using the NIH imaging program, version 1.63 (NIH, Bethesda, MD, USA).

Electrophoretic mobility shift assay (EMSA). Preparation of oligonucleotides and EMSAs were performed as described previously (19). Briefly, the following annealed 22-mer duplexes were prepared: 5'-GGTGGCCTGACXCATTCCC CAA-3' and 3'-ACCGGACTGYGTAAGGGGTTGG-5', where X=G or 8-oxo-dG and Y=A, C, G or T. Duplexes (22-mers) were end-labeled with [α-^{32}P]dCTP using the Klenow fragment for extension, and gel-purified. Half the volume of the labeled oligonucleotide without 8-oxo-dG was treated with 0.3 mM cisplatin at 37°C for 12 h, and then purified by ethanol precipitation. Purified GST fusion proteins were used directly in EMSAs. Reaction mixtures contained 5% glycerol, 10 mM Tris-HCl pH 7.5, 50 mM NaCl, 0.1 mM EDTA, 1 mM DTT, 0.4 ng/μl of ^{32}P-labeled probe DNA and the indicated amounts of GST fusion proteins, and were mixed. Binding reactions were incubated for 5 min at room temperature. Products were analyzed on 4% polyacrylamide gels in 0.5X Tris-borate EDTA buffer using a bioimaging analyzer (BAS 2000; Fuji Photo Film, Tokyo) (19).

Results

Both mtTFA and TRX2 are expressed in cisplatin-resistant cells. We previously showed that p53 interacts with mtTFA and enhances the DNA binding activity of mtTFA to cisplatin-damaged DNA, but inhibits its binding to oxidatively damaged DNA (22). Cisplatin induces both DNA damage and oxidative

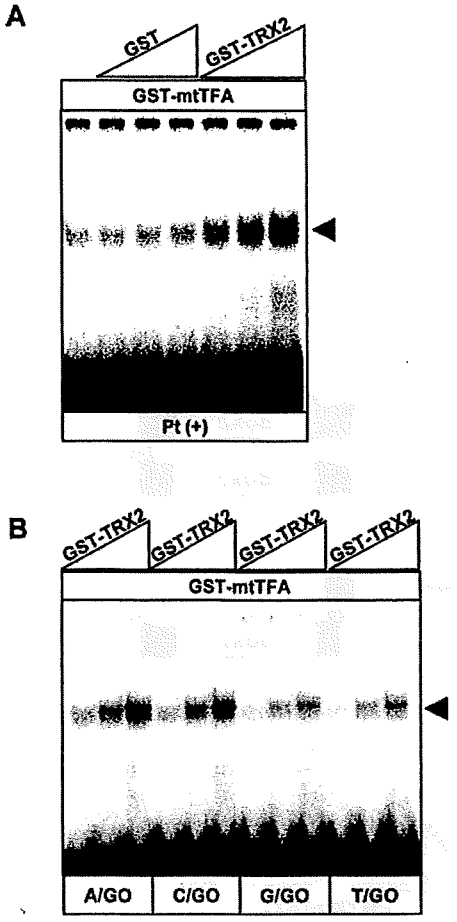

Figure 3. Effect of TRX2 on the binding of cisplatin-damaged or oxidatively damaged DNA by mtTFA. (A) Purified GST-mtTFA (90 ng) were mixed with GST or GST-TRX2 (10, 30 and 90 ng) and incubated with ^{32}P-labeled double-stranded oligonucleotides (0.4 ng/μl) containing cisplatin cross-linked. Binding complexes were subjected to EMSA. The arrowhead indicates DNA-protein complexes. (B) Effect of TRX2 on mtTFA binding to mismatch-containing oxidized oligonucleotides. Increasing amounts of GST-TRX2 (10, 30 and 90 ng) were mixed with GST-mtTFA (90 ng) and incubated with the indicated ^{32}P-labeled double-stranded oligonucleotides containing mismatches (A/GO, C/GO, G/GO and T/GO). Binding complexes were subjected to EMSAs. GO indicates 8-oxo-dG. The arrowhead indicates DNA-protein complexes.

stress in mitochondria and thioredoxin1 is upregulated in cisplatin resistant cells. Based on these previous results, we first examined the expression of mtTFA and the antioxidant protein TRX2 in cisplatin-resistant cells. The expression levels of both mtTFA and TRX2 were upregulated in cisplatin-resistant cells (Fig. 1).

Interaction of TRX2 with mtTFA. We then next investigated whether TRX2 interacts with mtTFA. As shown in Fig. 2A, mtTFA interacts with TRX2 *in vivo*. To confirm the association and binding site, we performed a pull-down assay using immobilized GST-fusion proteins comprising mtTFA deletion mutants and Flag-TRX2 (Fig. 2B). This assay demonstrated that the HMG box 1 motif of mtTFA directly participates in the interaction, but that the HMG box 2 motif does not (Fig. 2C).

Effect of TRX2 association on the binding of mtTFA to damaged DNA. We previously showed that the HMG box 1 motif possesses damaged DNA binding activity, but that the HMG box 2 motif does not (19). The interaction of mtTFA with TRX2 may alter the damaged DNA binding activity of mtTFA. An EMSA showed that GST-mtTFA can form a specific complex with cisplatin-damaged DNA and mismatch-containing DNA with 8-oxo dG. We observed that addition of TRX2 to the mtTFA-DNA binding reaction resulted in significant enhancement of binding of mtTFA to both cisplatin-damaged DNA and oxidatively damaged DNA (Fig. 3A and B).

mtTFA structure regulates the association with TRX2. It has been shown that mtTFA formed multimers under physiological conditions (27). To confirm whether the interaction of TRX2 with mtTFA requires a specific structure of mtTFA, we introduced mutations at two cysteine residues, positions 49 and 246, as shown in Fig. 4A. Pull-down assays showed that two mtTFA mutants, mtTFA-GC and mtTFA-CX, interacted with TRX2 with the same affinity as wild-type mtTFA-CC. However, the association of mtTFA with TRX2 was significantly enhanced when the mtTFA-GX mutant was used (Fig. 4B). This indicates that the cysteine-dependent secondary structure of mtTFA may regulate its association with TRX2. These mutants, as well as wild-type mtTFA, could bind to damaged DNA. Oxidized DNA binding was significantly increased when the mtTFA-GX mutant was used (Fig. 4C). The enhancement of the DNA binding activity of mtTFA by TRX2 was observed for all mtTFA mutants (Fig. 4D).

Discussion

In this study, we identified a novel interaction of mtTFA with TRX2. Cytosolic thioredoxin has a wide variety of biological activities (28). Thioredoxin participates in the regulation of apoptosis via a direct interaction with ASK1 and protects cells against oxidative stress (29). In addition to cytosolic TRX1, cells contain another TRX, TRX2, which is localized in mitochondria. Expression of the TRX1 and TRX2 genes is upregulated in cisplatin-resistant cells (30). Nuclear HMG box proteins are often upregulated in cisplatin-resistant cells (1). Here, we observed a significant increase in the levels of the mitochondrial HMG box protein mtTFA in cisplatin-resistant cells. Collectively, these data suggest a functional interaction between mtTFA and TRX2 because both proteins are localized in mitochondria. Mitochondria act as suppliers of ATP and produce ROS. On the other hand, mitochondria function as central players in modulating apoptosis. Little is known regarding the function of TRX2 and its potential role in apoptosis (31). It has been shown that overexpression of TRX2 makes cells resistant to etoposide (32). Our data also reveal that TRX2 expression is upregulated in cisplatin-resistant cells, consistent with the fact that drug-resistant cells often show apoptosis-resistant phenotypes. Similar results have previously been reported, such as the finding that both TRX1 and TRX2 expression are increased in doxorubicin-resistant ovarian cancer cells (33). Additionally, significantly increased levels of apoptosis have been observed in mtTFA-knockout mice, suggesting that mtTFA also plays an important

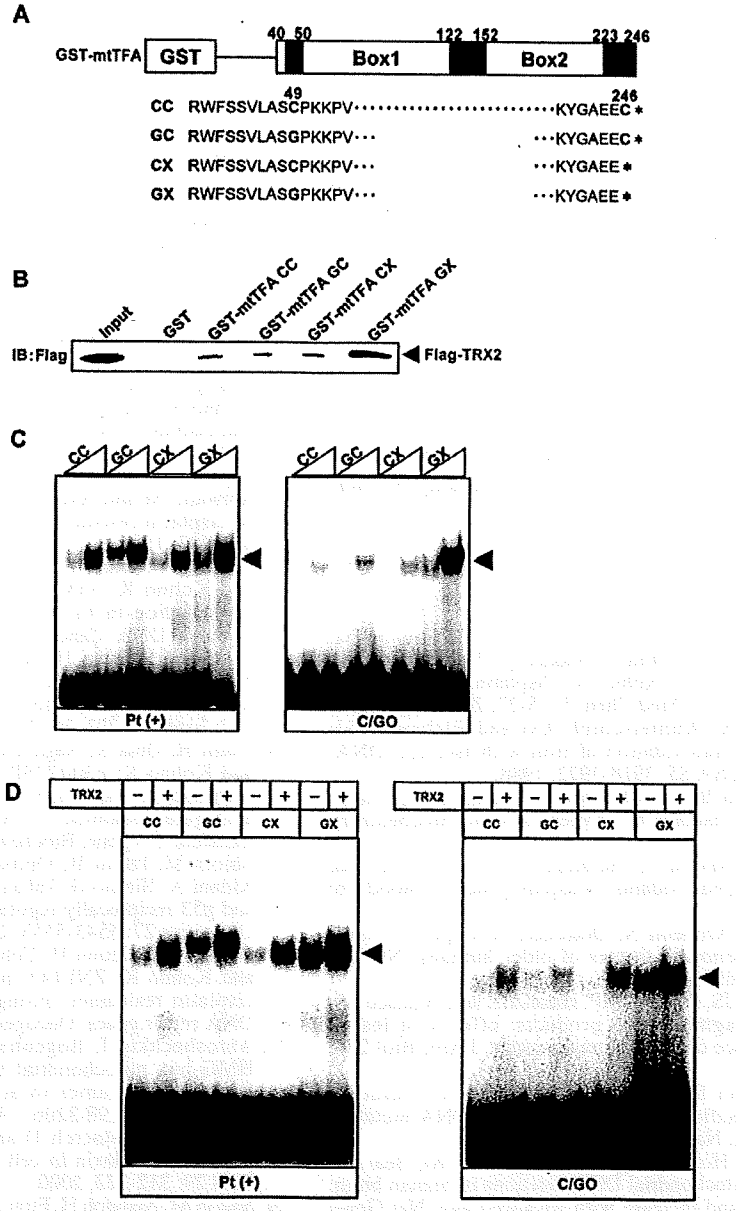

Figure 4. Effect of mtTFA mutation on binding to cisplatin-damaged or oxidized DNA. (A) Schematic representation of a GST-mtTFA fusion protein and its mutation of two cysteine residues (C49G and/or C246X). CC, GC, CX and GX indicate wild-type, C49G, C246X, C49G and C246X, respectively. (B) GST fusion proteins immobilized on glutathione-sepharose 4B beads were incubated with Flag-TRX2 expressed in bacteria. Bound protein samples representing 10% of the input were subjected to SDS-PAGE and Western blot analysis with anti-Flag antibody. (C) Purified GST fusion proteins (30 and 90 ng) were incubated with ^{32}P-labeled double-stranded oligonucleotides (0.4 ng/μl) containing cisplatin cross-linked or 8-oxo-dG (C/GO). Binding complexes were subjected to EMSAs. The arrowhead indicates DNA-protein complexes. (D) Purified GST fusion proteins (90 ng) were mixed with GST or GST-TRX2, and incubated with ^{32}P-labeled double-stranded oligonucleotides (0.4 ng/μl) containing cisplatin cross-linked or 8-oxo-dG (C/GO). Binding complexes were subjected to EMSAs. - and + indicate GST (90 ng) and GST-TRX2 (90 ng), respectively. The arrowhead indicates DNA-protein complexes.

role in apoptosis. mtTFA functions not only as a transcription factor, but also as DNA binding protein, like nuclear chromatin, to protect mtDNA from DNA damage. Fig. 2 shows that TRX2 supports the DNA binding activity of mtTFA to damaged DNA through a direct interaction.

We previously showed that both HMG box 1 and HMG box 2 motifs could interact independently with p53, which is localized to mitochondria under conditions of DNA damage stress (34). TRX2 interacts with the HMG box 1 motif of mtTFA (Fig. 2C). These findings indicate that mode of interaction of TRX2 with mtTFA is completely different from that of the interaction with p53 (22). Although there is some similarity in the primary amino acid sequences between HMG box 1 and HMG box 2, TRX2 only interacts with HMG box 1. This suggests that the secondary structure of mtTFA may modulate its association with TRX2. We then introduced mutations at two cysteine residues, positions 49 and 246 (Fig. 4A). The mutant mtTFA proteins could bind equally well to damaged DNA as wild-type mtTFA. However, the association of TRX2 with mtTFA was enhanced when the mtTFA-GX mutant was used. TRX2 can support DNA binding by mtTFA, even when a conformational change in mtTFA is

induced by ROS, suggesting that mtTFA can still bind and protect mtDNA under conditions of oxidative stress.

The physiological multimerization of mtTFA may efficiently support DNA binding to mtDNA. A conformational change in mtTFA might inhibit multimerization. Therefore, TRX2 can enhance the DNA binding activity of damaged mtTFA, which cannot form multimers, to protect mtDNA. Characterization of the interaction of TRX2 with mtTFA will aid our understanding of the mtTFA function in both normal and pathological conditions.

Acknowledgements

Grant support: This study was supported by KAKENHI (17016075), a UOEH Grant for Advanced Research, and The Vehicle Racing Commemorative Fundation. We thank Satoko Takazaki, Seiko Mifune and Saori Tabata for their technical assistance.

References

1. Torigoe T, Izumi H, Ishiguchi H, Yoshida Y, Tanabe M, Yoshida T, Igarashi T, Niina I, Wakasugi T, Imaizumi T, Momii Y, Kuwano M and Kohno K: Cisplatin resistance and transcription factors. Curr Med Chem 5: 15-27, 2005.
2. Loeb LA, James EA, Waltterscorph AM and Klebanoff SJ: Mutagenesis by the autoxidation of iron with isolated DNA. Proc Natl Acad Sci USA 85: 3918-3922, 1988.
3. McBride TJ, Preston BD and Loeb LA: Mutagenic spectrum resulting from DNA damage by oxygen radicals. Biochemistry 30: 207-213, 1991.
4. Weitzman SA and Gordon LI: Inflammation and Cancer: role of phagocyte-generated oxidants in carcinogenesis. Blood 76: 655-663, 1990.
5. Cortopassi GA and Arnheim N: Detection of a specific mitochondrial DNA deletion in tissues of older humans. Nucleic Acids Res 18: 6927-6933, 1990.
6. Maccabee M, Evans JS, Glackin MP, Hatahet Z and Wallace SS: Pyrimidine ring fragmentation products: effects of lesion structure and sequence context on mutagenesis. J Mol Biol 236: 514-530, 1994.
7. Soong NW, Hinton DR, Cortopassi G and Arnheim N: Mosaicism for a specific somatic mitochondrial DNA mutation in adult human brain. Nat Genet 2: 318-323, 1992.
8. Corral-Debrinski M, Horton T, Lott MT, Shoffner JM, Beal MF and Wallace DC: Mitochondrial DNA deletions in human brain: regional variability and increase with advanced age. Nat Genet 2: 324-329, 1992.
9. Polyak K, Li Y, Zhu H, Lengauer C, Willson JK, Markowitz SD, Trush MA, Kinzler KW and Vogelstein B: Somatic mutations of the mitochondrial genome in human colorectal tumours. Nat Genet 20: 291-293, 1998.
10. Habano W, Nakamura S and Sugai T: Microsatellite instability in the mitochondrial DNA of colorectal carcinomas: Evidence for mismatch repair systems in mitochondrial genome. Oncogene 17: 1931-1937, 1998.
11. Wallace DC: Mitochondrial diseases in man and mouse. Science 283: 1482-1488, 1999.
12. Parisi MA and Clayton DA: Similarity of human mitochondrial transcription factor 1 to high mobility group proteins. Science 252: 965-969, 1991.
13. Larsson NG, Wang J, Wilhelmsson H, Oldfors A, Rustin P, Lewandoski M, Barsh GS and Clayton DA: Mitochondrial transcription factor A is necessary for mtDNA maintenance and embryogenesis in mice. Nat Genet 18: 231-236, 1998.
14. Takamatsu C, Umeda S, Ohsato T, Ohno T, Abe Y, Fukuoh A, Shinagawa H, Hamasaki N and Kang D: Regulation of mitochondrial D-loops by transcription factor A and single-stranded DNA-binding protein. EMBO Rep 3: 451-456, 2002.
15. Pil PM and Lippard SJ: Specific binding of chromosomal protein HMG1 to DNA damaged by the anticancer drug cisplatin. Science 256: 234-237, 1992.
16. Hughes EN, Engelsberg BN and Billings PC: Purification of nuclear proteins that bind to cisplatin-damaged DNA: identity with high mobility group proteins 1 and 2. J Biol Chem 267: 13520-13527, 1992.
17. Billings PC, Davis RJ, Engelsberg BN, Skov KA and Hughes EN: Characterization of high mobility group protein binding to cisplatin-damaged DNA. Biochem Biophys Res Commun 188: 1286-1294, 1992.
18. Turchi JJ, Li M and Henkels KM: Cisplatin-DNA binding specificity of calf high-mobility group 1 protein. Biochemistry 35: 2992-3000, 1996.
19. Yoshida Y, Izumi H, Ise T, Uramoto H, Torigoe T, Ishiguchi H, Murakami T, Tanabe M, Nakayama Y, Itoh H, Kasai H and Kohno K: Human mitochondrial transcription factor A binds preferentially to oxidatively damaged DNA. Biochem Biophys Res Commun 295: 945-951, 2002.
20. Murakami T, Shibuya I, Ise T, Chen ZS, Akiyama S, Nakagawa M, Izumi H, Nakamura T, Matsuo K, Yamada Y and Kohno K: Elevated expression of vacuolar proton pump genes and cellular pH in cisplatin resistance. Int J Cancer 93: 869-874, 2001.
21. Fujii R, Mutoh M, Niwa K, Yamada K, Aikou T, Nakagawa M, Muwano M and Akiyama S: Active efflux system for cisplatin in cisplatin-resistant human KB cells. Jpn J Cancer Res 85: 426-433, 1994.
22. Yoshida Y, Izumi H, Torigoe T, Ishiguchi H, Itoh H, Kang D and Kohno K: p53 physically interacts with mitochondrial transcription factor A and differentially regulates binding to damaged DNA. Cancer Res 63: 3729-3734, 2003.
23. Uramoto H, Izumi H, Ise T, Tada M, Uchiumi T, Kuwano M, Yamamoto K, Funa K and Kohno K: p73 interacts with c-Myc to regulate Y-box-binding protein-1 expression. J Biol Chem 277: 31694-31702, 2002.
24. Izumi H, Ohta R, Nagatani G, Ise T, Nakayama Y, Nomoto M and Kohno K: p300/CBP-associated factor (P/CAF) interacts with nuclear respiratory factor-1 to regulate the UDP-N-acetyl-α-D-galactosamine: polypeptide N-acetylgalactosaminyl-transferase-3 gene. Biochem J 373: 713-722, 2003.
25. Shiota M, Izumi H, Onitsuka T, Miyamoto N, Kashiwagi E, Kidani A, Hirano G, Takahashi M, Naito S and Kohno K: Twist and p53 reciprocally regulate target genes via direct interaction. Oncogene 27: 5543-5553, 2008.
26. Wakasugi T, Izumi H, Uchiumi T, Suzuki H, Arao T, Nishio K and Kohno K: ZNF143 interacts with p73 and is involved in cisplatin resistance through the transcriptional regulation of DNA repair genes. Oncogene 26: 5194-5203, 2007.
27. Antoshechkin I, Bogenhagen DF and Mastrangelo IA: The HMG-box mitochondrial transcription factor xl-mtTFA binds DNA as a tetramer to activate bidirectional transcription. EMBO J 16: 3198-3206, 1997.
28. Powis G, Mustacich D and Coon A: The role of the redox protein thioredoxin in cell growth and cancer. Free Radic Biol Med 29: 312-322, 2000.
29. Saitoh M, Nishitoh H, Fujii M, Takeda K, Tobiume K, Sawada Y, Kawabata M, Miyazono K and Ichijo H: Mammalian thioredoxin is a direct inhibitor of apoptosis signal-regulating kinase (ASK) 1. EMBO J 17: 2596-2606, 1998.
30. Yokomizo A, Ono M, Nanri H, Makino Y, Ohga T, Wada M, Okamoto T, Yodoi J, Kuwano M and Kohno K: Cellular levels of thioredoxin associated with drug sensitivity to cisplatin, mitomycin C, doxorubicin, and etoposide. Cancer Res 55: 4293-4296, 1995.
31. Patenaude A, Murthy MRV and Mirault ME: Mitochondrial thioredoxin system; effects of TrxR2 overexpression on redox balance, cell growth, and apoptosis. J Biol Chem 279: 27302-37314, 2004.
32. Damdimopoulos AE, Vizuete AM, Huikko MP, Gustafsson JA and Spyrou G: Human mitochondrial thioredoxin; involvement in mitochondrial membrane potential and cell death. J Biol Chem 277: 33249-33257, 2002.
33. Kalinina EV, Chernov NN, Saprin AN, Kotova YN, Gavrilova YA, Chermnykh NS and Shcherbak NP: Expression of genes for thioredoxin1 and thioredoxin2 in multidrug resistance ovarian carcinoma cells SKVLB. Bull Exp Biol Med 144: 301-303, 2007.
34. Imamura T, Izumi H, Nagatani G, Ise T, Nomoto M, Iwamoto Y and Kohno K: Interaction with p53 enhances binding of cisplatin-modified DNA by high mobility group 1 protein. J Biol Chem 276: 7534-7540, 2001.

Nuclear Y-Box Binding Protein-1, a Predictive Marker of Prognosis, Is Correlated with Expression of HER2/ErbB2 and HER3/ErbB3 in Non-small Cell Lung Cancer

Masaki Kashihara, MD,† Koichi Azuma, MD, PhD,‡ Akihiko Kawahara, PhD,§ Yuji Basaki, PhD,*‖ Satoshi Hattori, PhD,¶ Takashi Yanagawa, PhD,¶ Yasuhiro Terazaki, MD, PhD,‡ Shinzo Takamori, MD, PhD,‡ Kazuo Shirouzu, MD, PhD,‡ Hisamichi Aizawa, MD, PhD,‡ Kenji Nakano, MD, PhD,‖ Masayoshi Kage, MD, PhD,§Michihiko Kuwano, MD, PhD,‖ and Mayumi Ono, PhD,*‖*

Introduction: Nuclear expression of Y-box binding protein-1 (YB-1) is closely associated not only with global drug resistance and expression of several growth factor receptors in various human malignancies but also with overall patient survival.

Methods: The effect of YB-1 knockdown on expression of epidermal growth factor receptor (EGFR) family proteins was examined by Western blot using human lung cancer cell lines. Immunohistochemistry was used to evaluate the expression of nuclear YB-1 and EGFR family proteins in patients with non-small cell lung cancer (NSCLC) (n = 104).

Results: In the five NSCLC cell lines, expressions of EGFR, human epidermal growth factor receptor 2 (HER2), HER3, and hepatocyte growth factor receptor (c-Met) in PC-9 cells; of HER2 and c-Met in EBC-1 cells; and of HER3 in QG56 cells were down-regulated by YB-1 knockdown. By immunohistochemical analysis, we observed that HER3 expression was significantly negatively correlated with nuclear YB-1 expression in squamous cell carcinoma (p = 0.038). HER2 expression was positively correlated with nuclear YB-1 expression in adenocarcinoma (p = 0.052). Nuclear expression of YB-1 correlated with overall survival of all patients (p = 0.028) and of patients with adenocarcinoma (p = 0.007). Furthermore, there was a significant difference in therapeutic efficacies of gefitinib between patients with nuclear YB-1 expression and those with non-nuclear YB-1 expression in patients with NSCLC (p = 0.004, n = 26) but not between those with high and those with low expression of EGFR, HER2, HER3, and c-Met.

Conclusion: Nuclear YB-1 expression might be essential for the malignant phenotype in lung cancer patients and might be an important biomarker for the development of therapeutic strategy against NSCLC.

Key Words: YB-1, NSCLC, HER2, HER3.

(*J Thorac Oncol.* 2009;4: 1066–1074)

The Y-box binding protein-1 (YB-1), whose cold shock domain is highly conserved, plays essential roles in DNA damage repair and in both transcriptional and translational regulation of various genes in nucleus and cytoplasm.[1,2] In the nucleus, YB-1 recognizes DNA damage induced by cisplatin and radiation and promotes transcription of drug-resistance relevant genes such as *MDR1/ABCB1*, a representative multidrug resistance-related ATP-binding cassette transporter, and major vault protein/lung resistance-related protein, a drug-resistance-related vault protein, suggesting the applicability of YB-1 as a global biomarker of drug resistance.[2,3] Moreover, nuclear expression of YB-1 significantly correlates with the survival of patients with various malignancies, including ovarian cancer,[4,5] synovial sarcoma and rhabdomyosarcoma,[6,7] lung cancer,[8] breast cancer,[9] and pediatric glioblastoma.[10] Most of these patients show a close association of nuclear YB-1 expression with poor prognosis, irrespective of treatment modality. It is likely that multiple tumor characteristics, including growth and metastasis/invasion as well as acquisition of global drug resistance, cause YB-1 expression to be associated with poor prognosis in cancer patients.

Nuclear expression of YB-1 is promoted through PI3K/Akt signaling in human breast and ovarian cancer cells in response to growth stimulation,[11,12] and YB-1 knockdown suppresses expression of DNA replication-related and growth/cell cycle-related genes as well as growth factor genes.[12,13] YB-1 gene knock-in promotes development of breast cancer of various histologic types in animal models, suggesting that YB-1 is a breast cancer oncogene.[14] YB-1

*Department of Pharmaceutical Oncology, Graduate School of Pharmaceutical Sciences, Kyushu University, Fukuoka, Japan; †Department of Surgery, Kurume University, Kurume, Japan; ‡Division of Respirology, Neurology, and Rheumatology, Department of Internal Medicine, Kurume University School of Medicine, Kurume, Japan; §Department of Pathology, Kurume University Hospital, Kurume, Japan; and ¶Biostatistics Center, Kurume University, Kurume, Japan; ‖Innovation Center for Medical Redox Navigation, Kyushu University, Fukuoka, Japan.

Disclosure: The authors declare no conflicts of interest.

Address for correspondence: Mayumi Ono, PhD, Department of Pharmaceutical Oncology, Graduate School of Pharmaceutical Sciences, Kyushu University, 3-1-1, Maidashi, Higashi-ku, Fukuoka, 812-8582, Japan. E-mail: mono@phar.kyushu-u.ac.jp

ISSN: 1556-0864/09/0409-0001

knockdown in mice causes embryonic lethality and severe growth retardation.[15,16] Furthermore, YB-1 overexpression induces epidermal growth factor (EGF)-independent growth through constitutive EGF receptor (EGFR) activation in human mammary cells in vitro.[17] Wu et al.[18] reported that the introduction of an Akt-activation-insensitive mutation into YB-1 caused a marked decrease in the expression of both EGFR and human epidermal growth factor receptor 2 (HER2), suggesting a close linkage between YB-1 and expression of EGFR and HER2 in breast cancer cells in vitro. YB-1 knockdown also results in markedly decreased expression of EGFR and HER2 in some human breast cancer cell lines in culture.[9] Taken together, these basic studies in vitro and in vivo strongly suggest that YB-1 is closely involved in EGF/transforming growth factor-α-dependent and -independent tumor growth and carcinogenesis in cancer.

The clinical study by Janz et al.[19] was the first to demonstrate the close association of nuclear YB-1 expression with HER2 expression in primary breast cancers. This correlation with the expression of EGFR and HER2 in patients with breast cancer ($n = 389$) was further supported by array studies with tumor tissue.[18] Of various genes, including *EGFR*, *HER2*, *ERα*, *ERβ*, and *CXCR4*, that could be affected by YB-1 knockdown in vitro, biostatistical analysis showed that YB-1 nuclear expression was positively associated with the expression of HER2 and negatively associated with the expression of CXCR4 and ERα.[9] A recent study by Stratford et al.[20] also showed the possible involvement of YB-1 in the therapeutic efficacy of an EGFR-targeting drug, gefitinib, in basal-like breast cancer. These findings suggest that YB-1 may play a key role in the expression of cell growth-related genes, including EGFR family genes, in breast cancer cells and may also modulate the therapeutic efficacy of EGFR family targeting drugs.

In this study, we determined the relationship between YB-1 expression and that of several growth factor receptors, EGFR, HER2, HER3, hepatocyte growth factor receptor (c-Met), and insulin-like growth factor 1 receptor (IGF-1R), in human lung cancer cell lines in culture. Moreover, we determined whether nuclear YB-1 expression was correlated with the expression of EGFR, HER2, HER3, c-Met, and phosho Akt (pAkt) in tumor tissue from patients with non-small cell lung cancer (NSCLC), and also whether therapeutic efficacy of gefitinib was correlated with nuclear YB-1 expression. We discuss the clinical and immunohistochemical characteristics of NSCLC with particular reference to the absence or presence of nuclear YB-1 expression and the expression of EGFR family proteins.

MATERIALS AND METHODS

Cell Lines and Reagents

PC-9, QG56, and 11_18 were cultured in Roswell Park Memorial Institute (culture medium) supplemented with 10% fetal bovine serum. A549 and EBC-1 were cultured in Dulbecco's minimum essential medium supplemented with 10% fetal bovine serum. Anti-YB-1 was generated as described previously.[21] Anti-EGFR, IGF-1R, Akt, pAkt, Erk, and pErk antibodies were obtained from Cell Signaling Technology (Beverly, MA). Anti-HER2 was purchased from Upstate, Inc. (Lake Placid, NY). Antic-Met and anti-HER3 were obtained from Santa Cruz Biotechnology, Inc. (Santa Cruz, CA). Anti-GAPDH was purchased from TREVIGEN (Gaithersburg, MD).

Small Interfering RNA Transfection and Immunoblotting

The small interfering RNA (siRNA) corresponding to the nucleotide sequence of YB-1 was purchased from QIAGEN.[9] SiRNA duplexes were transfected with Lipofectamine RNAiMAX and Opti-MEM medium (Invitrogen, Carlsbad, CA) according to the manufacturer's recommendations. Forty-eight hours after siRNA transfection, cells were lysed in cold protein extraction reagent (M-PER; PIERCE, Rockford, IL) with protease inhibitors and phosphatase inhibitors. Nuclear and cytoplasmic fractions were prepared as described previously.[12] Lysates were subjected to SDS-PAGE and blotted onto Immobilon membrane (Millipore Corp., Bedford, MA). After transfer, the membrane was incubated with the primary antibody and visualized with secondary antibody coupled to horseradish peroxidase and enhanced chemiluminescence Western Blotting Detection Reagents (GE Healthcare, Piscataway, NJ). For cell proliferation assay, 2.5×10^4 cells were seeded in 24-well plates (IWAKI, Tokyo, Japan) and cell number in each well was counted at 96 hours after transfection of siRNA.

Patients and Tumor Samples

We examined 104 patients with primary NSCLC whose tumors had been completely surgically removed in the Department of Surgery of Kurume University between 1997 and 2004. Among the 104 patients, 66 patients were diagnosed histologically as having adenocarcinoma and the other 38 patients were diagnosed as having squamous cell carcinoma. The age of the patients with NSCLC ranged from 41 to 82 years (median, 66 years). Of the total number of patients, 67 were men and 37 were women. The median follow-up was 1511.5 days with a range of 159 to 3801 days. Of these patients, 26 patients received gefitinib against recurrent disease after surgical resection between June 2003 and September 2008 with the median interval between operation and gefitinib treatment of 760 days (range, 225-3062 days). Five patients were treated with gefitinib as an initial therapy and the others were treated with gefitinib as a second- or a third-line therapy (21 patients, platinum doublets as first line; five patients, monotherapy, nonplatinum doublets, and platinum doublets as second line).

Immunohistochemistry

Paraffin-embedded tissue samples were cut at 4 μm, placed on coated glass slides, and labeled with the following antibodies by the BenchMark XT (Ventana Automated Systems, Inc., Tucson, AZ) or ChemMate ENVISION (DakoCytomation, Glostrup, Denmark) methods: YB-1, EGFR, HER2, HER3, pAkt, and c-Met. The BenchMark XT method was used for YB-1, EGFR, HER2, and HER3. This automated system used the streptavidin biotin complex method with DAB as chromogen (Ventana iVIEW DAB Detection Kit). Antigen retrieval of YB-1 and HER2 was performed by heat treatment in CC1 (Ventana, Inc.) and that of EGFR and HER3 was performed by protease treatment (protease K, Ventana, Inc.). The ChemMate ENVISION method was used for pAkt and c-Met. Endogenous

peroxidase activity was inhibited by incubating the slides in 3% H_2O_2 for 5 minutes. Each slide was incubated overnight with the antibody at 4°C. For staining detection, DAB was used as chromogen. The samples were viewed using an Olympus BX51 microscope (Olympus, Tokyo, Japan).

Expression of YB-1 protein with variable intensity showed in the nuclei and/or cytoplasm with variable intensity. Only nuclei of cancer cells with strong expression were interpreted as positive. Expression of EGFR and HER2 was classified into four categories: score 0, no staining at all or weak membrane expression in <10% of cancer cells; score 1+, weak expression in >10% of cancer cells; score 2+, weak to moderate expression on the entire membrane in >10% of the cancer cells; and score 3+, strong expression on the entire membrane in >10% of cancer cells. HER3, pAkt, and c-Met were classified into the same four categories but the localization of expression included both membrane and cytoplasm. The scoring of immunohistochemistry (IHC) was defined as follows in order that the difference in the number of patients in two categories of negative and positive were as small as possible. The expressions of HER2 and pAkt were defined as follows: scores of 2+ or 3+ were regarded as positive and scores of 0 or 1were regarded as negative. The expression of IHC for EGFR, HER3, and c-Met was defined as follows: score of 3+ was regarded as positive and scores of 0, 1, or 2+ were regarded as negative. All IHC studies were evaluated by two IHC-experienced reviewers (A.K. and M.K.) who were blinded to the clinical status of the patients.

Statistical Analysis

Associations between histologic type and clinicopathologic findings (age, gender, smoking status, stage, and histologic differentiation) and molecular markers (EGFR, HER2, HER3, c-Met, and pAkt) were tested by Fisher's exact test. Associations between YB-1 and clinicopathologic findings and other molecular markers were tested in similar ways. A p value <0.05 was regarded as statistically significant unless indicated. The overall survival was defined as time to death because of any case from the date of surgical operation. The relationships between overall survival and YB-1 expression, and other clinicopathologic findings and molecular markers, were examined by the Kaplan-Meier method and the log-rank test. Hazard ratios (HRs) were estimated by Cox regressions. Adjusted HRs for possible confounding factors were also estimated by applying the Cox regression models with the factors as explanatory variables. Twenty-six patients were treated with gefitinib after progressive disease. Time to further progressive disease from initiation of gefitinib treatment was evaluated for these patients. The effect of YB-1 on the further progressive disease in the presence of gefitinib was examined in an exploratory matter by the Kaplan-Meier method and the log-rank test. Statistical analysis was performed with SAS version 9.1 (SAS Institute, Inc., Cary, NC) and revised version 2.7.0.

RESULTS

Knockdown of YB-1 and Expression of the EGFR, HER2, HER3, and c-Met Genes in NSCLC Cell Lines

We examined expression of the growth factor receptors EGFR, HER2, HER3, c-Met, and IGF-1R in five NSCLC cell lines. Expression of YB-1 was observed in both total cell fraction and nucleus in all the five NSCLC cell lines, although expression of YB-1 in both fractions of PC-9 and EBC-1 cells was only about 20% or less than that in the other three lines (Figures 1*A*, *B*). Expression levels of EGFR,

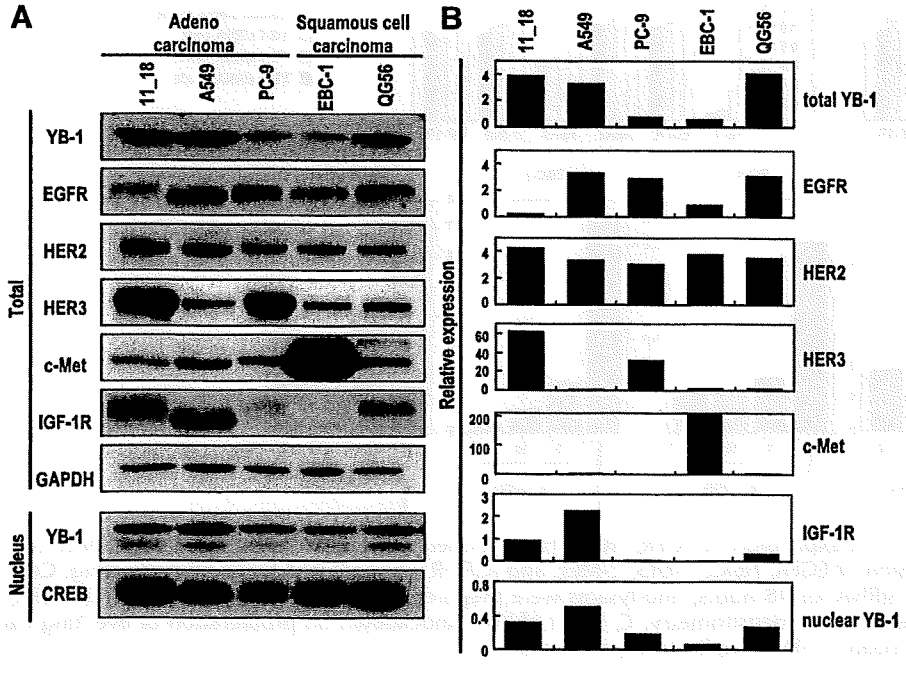

FIGURE 1. Expression of YB-1, EGFR, HER2, HER3, c-Met, and IGF-1R in human lung cancer cells. *A*, Expression of total and nuclear YB-1, EGFR, HER2, HER3, c-Met, and IGF-1R was determined by immunoblotting conducted on protein lysates extracted from these cell lines. Detection of GAPDH served as a loading control. *B*, Levels of total and nuclear YB-1, EGFR, HER2, HER3, c-Met, and IGF-1R expression were measured by densitometry.

HER2, HER3, c-Met, and IGF-1R varied among the five cell lines. Among the various cell lines, the two lines (PC-9 and EBC-1) with relatively low levels of YB-1 in the nucleus contained much lower amounts of IGF-1R protein than did the other three lines. However, expression of the other receptors (EGFR, HER2, HER3, and c-Met) was not significantly associated with expression levels of YB-1 in nucleus or total cell fraction of any of the cell lines. We next compared protein expression levels in the five NSCLC cell lines after treatment with YB-1 siRNA (Figure 2). Western blot analysis showed that YB-1 siRNA decreased protein levels of YB-1 in all five NSCLC cell lines. YB-1 knockdown resulted in decreased expression of EGFR in PC-9, of HER2 in PC-9 and EBC-1, of HER3 in PC-9 and QG56, and of c-Met in PC-9

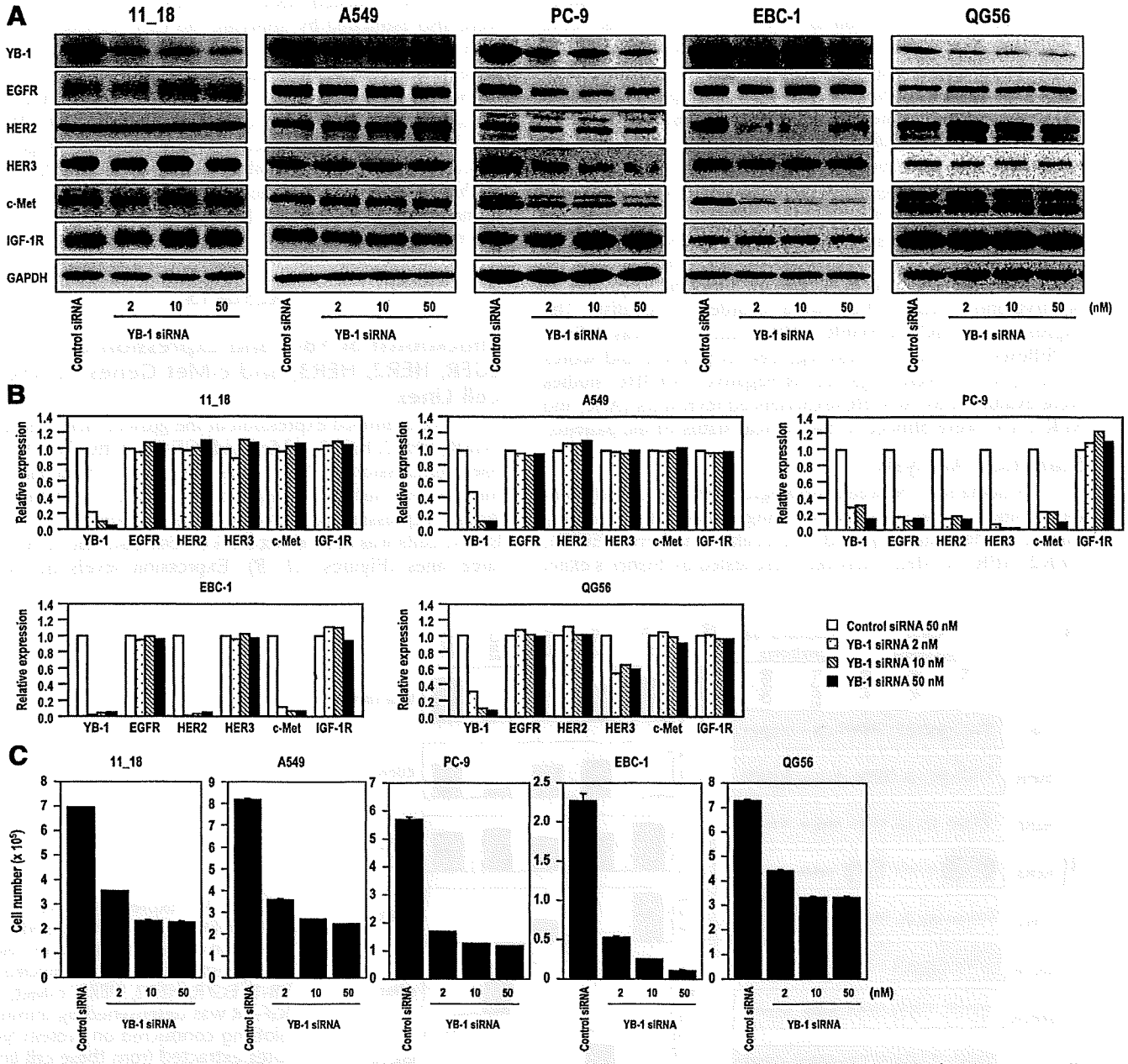

FIGURE 2. Effect of YB-1 knockdown on expression of EGFR, HER2, HER3, c-Met, and IGF-1R in human lung cancer cells. *A*, Effect of YB-1 knockdown on expression of EGFR, HER2, HER3, c-Met, and IGF-1R was analyzed by immunoblotting. Cells were incubated with control or YB-1 siRNA for 48 hours, and lysates were prepared. *B*, Levels of YB-1, EGFR, HER2, HER3, c-Met, and IGF-1R expression were measured by densitometry. *C*, Effect of YB-1 knockdown on proliferation of five lung cancer cell lines. Data are expressed as the mean ± SD of triplicate experiments.

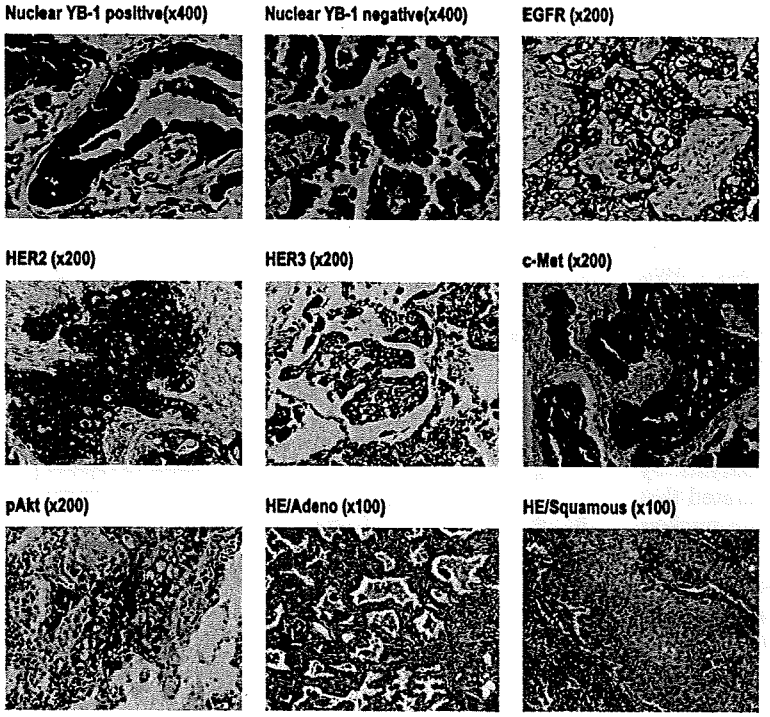

FIGURE 3. Histologic findings and expression of YB-1, EGFR, HER2, HER3, c-Met, and pAkt in human lung cancer. YB-1 expression was assessed as two patterns: nuclear positive or negative. Cancer cells showed strong expression of EGFR, HER2, HER3, and c-Met in the membrane. Moderate-to-strong expression of pAkt was found in the cytoplasm.

TABLE 1. Correlation Between Nuclear YB-1 Expression and Expression of Five Target Genes in Adenocarcinoma and Squamous Cell Carcinoma of NSCLC

	Adenocarcinoma							Squamous Cell Carcinoma						
			Nuclear YB-1							Nuclear YB-1				
			Negative		Positive					Negative		Positive		
Variables	*n*	%	*n*	%	*n*	%	*p*	*n*	%	*n*	%	*n*	%	*p*
EGFR														
Negative	42	63.6	30	63.8	12	63.2	1.000	25	65.8	10	76.9	15	60.0	0.473
Positive	24	36.4	17	36.2	7	36.8		13	34.2	3	23.1	10	40.0	
HER2														
Negative	60	90.9	45	95.7	15	78.9	0.052	36	94.7	11	84.6	25	100.0	0.111
Positive	6	9.1	2	4.3	4	21.1		2	5.3	2	15.4	0	0.0	
HER3														
Negative	37	56.1	26	55.3	11	57.9	1.000	33	86.8	9	69.2	24	96.0	0.038
Positive	29	43.9	21	44.7	8	42.1		5	13.2	4	30.8	1	4.0	
c-Met														
Negative	47	71.2	34	72.3	13	68.4	0.770	35	92.1	11	84.6	24	96.0	0.265
Positive	19	28.8	13	27.7	6	31.6		3	7.9	2	15.4	1	4.0	
pAkt														
Negative	41	62.1	29	61.7	12	63.2	1.000	27	71.1	9	69.2	18	72.0	1.000
Positive	25	37.9	18	38.3	7	36.8		11	28.9	4	30.8	7	28.0	

YB-1, Y-box binding protein-1; NSCLC, non-small cell lung cancer; EGFR, epidermal growth factor receptor.

and EBC-1. Of the five lines, expression of growth factor receptors was particularly susceptible to siRNA-dependent down-regulation in PC-9 and EBC-1 cells, which contain relatively lower levels of YB-1. However, we did not observe decreased expression of growth factor receptor proteins by YB-1 knockdown in 11_18 and A549 cells (Figures 2*A*, *B*). Overall, the reduced expression of EGFR family proteins and c-Met protein by YB-1 knockdown in some NSCLC cell lines suggests an association between YB-1 levels and expression of EGFR family proteins or c-Met protein. In addition, proliferation of

NSCLC cell lines was markedly suppressed to a similar extent in all five cell types, by 2 to 50 nmol/L of YB-1 siRNA (Figure 2C).

Association of Nuclear YB-1 Expression with Expression of EGFR, HER2, HER3, c-Met, and pAkt in NSCLC

To examine which genes are specifically associated with nuclear YB-1 localization in human NSCLC, we selected five molecular markers: EGFR, HER2, HER3, c-Met, and pAkt. Representative immunohistochemical staining patterns are shown in Figure 3. Expression of nuclear YB-1 was detected in 44 of 104 patients. Table 1 shows the results of Fisher's exact test for association between YB-1 and each of the molecular markers in adenocarcinoma and squamous cell carcinoma. To avoid misinterpretations arising from Simpson's paradox,[22] we emphasis on analysis by histologic differentiation. Such analysis demonstrated that there was significant negative correlation between nuclear expression of YB-1 and expression of HER3 in patients with squamous cell carcinoma ($p = 0.038$). There was also a trend to a correlation between nuclear expression of YB-1 and expression of HER2 in patients with adenocarcinoma ($p = 0.052$).

Nuclear YB-1 Expression and Survival of Patients with NSCLC

The estimated product-limit survival functions of nuclear YB-1 are shown in Figure 4, and the results of log-rank tests and unadjusted HRs are given in Table 2. Survival curves for patients with positive nuclear YB-1 expression were significantly different from those with negative expression (HR = 1.73; 95% confidence interval [CI] 1.05–2.83; $p = 0.028$). Further analysis showed that positive nuclear YB-1 expression significantly affected survival in adenocarcinoma (HR = 2.40; 95% CI 1.25–4.58; $p = 0.007$) but not in squamous cell carcinoma (HR = 1.50; 95% CI 0.60–3.72; $p = 0.381$; Table 2).

Adjusted HRs for patients with positive nuclear YB-1 expression relative to those with negative nuclear YB-1 expression were obtained by applying the Cox regression models with sex, smoking status, and histologic type as explanatory variables (Table 3). Stage was not adjusted in the Cox regression model, because it might be an intermediate variable between YB-1 expression and overall survival.[23] The adjusted HR was statistically significantly different from unity (HR = 1.96; 95% CI 1.13–3.38; $p = 0.016$) indicating that nuclear YB-1 expression affects overall survival even after adjusting for possible confounding factors. The Cox regression models with sex and smoking status were also applied separately by histologic type to determine the interaction between nuclear YB-1 and histologic type. Adjusted HRs for YB-1 expression were similar between adenocarcinoma and squamous cell carcinoma, although they were statistically significant only for patients with adenocarcinoma (HR = 2.19; 95% CI 1.12–4.28; $p = 0.022$ for adenocarcinoma, and HR = 2.14; 95% CI 0.74–6.15; $p = 0.158$ for squamous cell carcinoma).

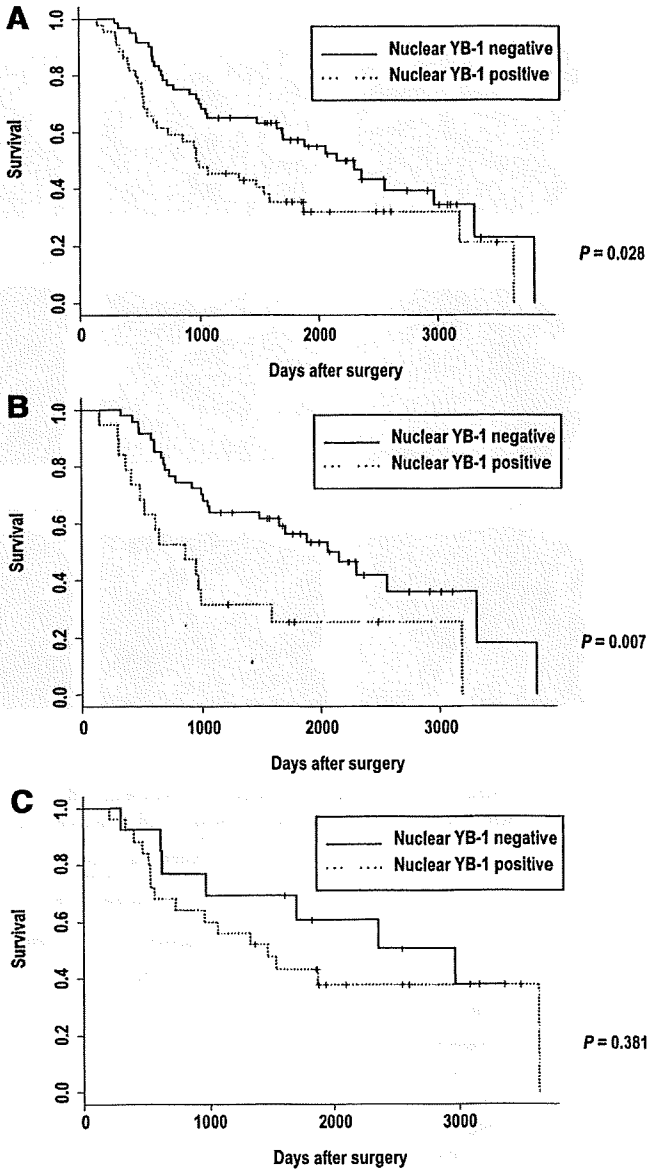

FIGURE 4. Kaplan-Meier plots of overall survival according to nuclear YB-1 expression in 104 patients with lung cancer. *A*, Total patients with NSCLC ($n = 104$), (*B*) patients with adenocarcinoma ($n = 66$), and (*C*) patients with squamous cell carcinoma ($n = 38$).

Nuclear YB-1 Expression and Therapeutic Efficacy of Gefitinib

Twenty-six patients administrated gefitinib after progressive disease. Among 26 patients, 24 patients were histologically diagnosed adenocarcinoma and other two patients were diagnosed squamous cell carcinoma. Eight of them were men and 18 were women. Seven of them were smoker and 19 were nonsmoker. The estimated product-limit survival functions of nuclear YB-1 for time to further disease progression from the initiation of gefitinib treatment are shown in Figure 5. Although patients' number for gefitinib treatment was

TABLE 2. Univariate Analysis of Patients Characteristics and Expression of Nuclear YB-1 and Other Target Genes in Relation to Regarding Overall Survival

	Adenocarcinoma			Squamous Cell Carcinoma			Total		
		Overall Survival			Overall Survival			Overall Survival	
Variables	*n*	HR (95% CI)	*p*	*n*	HR (95% CI)	*p*	*n*	HR (95% CI)	*p*
YB-1									
Negative	47	1.00	0.007	13	1.00	0.381	60	1.00	0.028
Positive	19	2.40 (1.25–4.58)		25	1.50 (0.60–3.72)		44	1.73 (1.05–2.83)	
EGFR									
Negative	42	1.00	0.098	25	1.00	0.190	67	1.00	0.701
Positive	24	1.71 (0.90–3.23)		13	0.52 (0.19–1.41)		37	1.11 (0.66–1.87)	
HER2									
Negative	60	1.00	0.566	36	1.00	0.005[a]	96	1.00	0.130
Positive	6	1.36 (0.48–3.86)		2	6.89 (1.45–32.7)		8	1.91 (0.82–4.47)	
HER3									
Negative	37	1.00	0.173	33	1.00	0.468	70	1.00	0.155
Positive	29	0.64 (0.33–1.23)		5	0.59 (0.14–2.52)		34	0.66 (0.38–1.17)	
c-Met									
Negative	47	1.00	0.528	35	1.00	0.645	82	1.00	0.428
Positive	19	1.24 (0.64–2.40)		3	1.41 (0.33–6.12)		22	1.27 (0.71–2.27)	
pAkt									
Negative	41	1.00	0.540	27	1.00	0.087	68	1.00	0.128
Positive	25	0.82 (0.42–1.57)		11	0.40 (0.13–1.19)		36	0.65 (0.38–1.14)	

[a] Significance of HER2 for squamous cell carcinoma may be artefactual obtained since only 2 patients with HER2 positive were observed and they happened to have extremely short overall survival by chance.

95% CI, 95% confidence interval; HR, hazard ratio; YB-1, Y-box binding protein-1; EGFR, epidermal growth factor receptor.

TABLE 3. Cox Regression Analysis for Overall Survival

	Adenocarcinoma		Squamous Cell Carcinoma		Total	
	HR (95% CI)	*p*	HR (95% CI)	*p*	HR (95% CI)	*p*
YB-1						
Negative	1.00	0.022	1.00	0.158	1.00	0.016
Positive	2.19 (1.12–4.28)		2.14 (0.74–6.15)		1.96 (1.13–3.38)	
Gender						
Negative	1.00	0.218	1.00	0.764	1.00	0.380
Positive	1.77 (0.63–5.03)		0.71 (0.17–3.64)		1.51 (0.61–3.75)	
Smoking						
Negative	1.00	0.726	1.00	0.414	1.00	0.655
Positive	0.83 (0.29–2.39)		0.47 (0.08–2.88)		0.81 (0.31–2.07)	
Histological						
Squamous					1.00	0.248
Adenocarcinoma					1.43 (0.78–2.65)	

95% CI, 95% confidence interval; HR, hazard ratio; YB-1, Y-box binding protein-1.

limited, the survival curves for patients with positive nuclear YB-1 expression and those with negative expression are quite distinct with statistical significance ($p = 0.004$).

DISCUSSION

Wu et al.[18] used array studies to establish a close correlation between total YB-1 expression and EGFR and HER2 expression in tumor tissue from patients with breast cancer. Our recent immunohistochemical analysis demonstrated that nuclear YB-1 expression is positively correlated with HER2, and negatively correlated with ERα and CXCR4, but not with EGFR in breast cancer clinical specimens.[9] In this study, YB-1 knockdown in five NSCLC cell lines caused down-regulation of EGFR, HER2, HER3, and c-Met in PC-9; of HER3 and c-Met in EBC-1; and of HER3 in QG56. There was no change in expression of growth factor receptor family proteins in the other two cell lines. However, cell proliferation was markedly suppressed by YB-1 knockdown in all five cell lines suggesting that YB-1 siRNA-induced inhibition of cell proliferation might not involve attenuation of these growth factor receptors. The underlying mechanism of YB-1 siRNA-induced growth inhibition in these cell lines remains

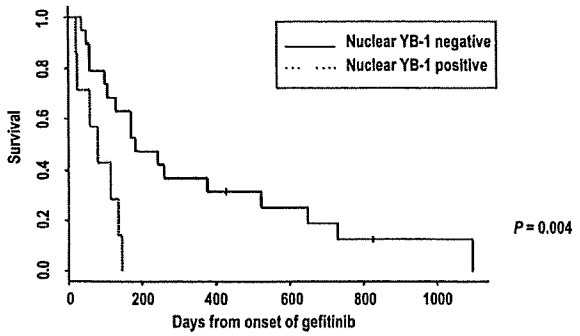

FIGURE 5. Kaplan-Meier estimate for time to further progressive disease from the initiation of gefitinib according to nuclear YB-1 expression in 26 patients treated with gefitinib after progressive disease.

unknown. Immunohistochemical analysis of clinical samples of NSCLC showed that nuclear YB-1 expression was negatively correlated with HER3 expression in squamous cell carcinoma ($p = 0.038$) and positively correlated with HER2 expression in adenocarcinoma ($p = 0.052$). However, nuclear YB-1 expression was not significantly correlated with EGFR or c-Met expression in either squamous cell carcinoma or adenocarcinoma.

Overexpression of HER2 in an NSCLC cell line with very low EGFR and high HER3 expression levels sensitizes these cells to growth inhibition by the EGFR-targeting drug gefitinib, and gefitinib abrogated formation of HER2/HER3 heterodimers.[24] Consistent with this report, there is a strong correlation between HER3 expression and sensitivity to gefitinib.[25] Another EGFR-targeting drug, erlotinib, also inhibits HER2 tyrosine kinase, and HER2/HER3 heterodimer formation sensitizes lung cancer cells to growth inhibition by erlotinib.[26] Taken together, expression of HER2 and HER3 coupled with formation of their heterodimers plays a critical role in determining the therapeutic efficacy of the EGFR-targeting drugs gefitinib and erlotinib.[27,28] The possible link between nuclear YB-1 expression and HER2 expression in adenocarcinoma ($p = 0.052$) might be in part responsible for the correlation between nuclear YB-1 expression and survival of patients with adenocarcinoma NSCLC. Nuclear YB-1 expression is positively correlated with HER2 expression in patients with breast cancer ($p = 0.015$).[9] Thus, HER2 expression could be modulated by nuclear YB-1 expression not only in patients with breast cancer[9] but also in patients with adenocarcinoma NSCLC (this study). HER3 expression was inversely correlated with nuclear expression of YB-1 in squamous cell carcinoma ($p = 0.038$), but HER3 expression alone did not correlate with survival of patients with NSCLC or of the subset with squamous cell carcinoma. It seems unlikely that the inverse correlation of nuclear YB-1 expression with HER3 expression is a factor in the poor prognosis associated with nuclear YB-1 expression in patients with squamous NSCLC.

In addition to the effect of altering the status of EGFR family proteins on the therapeutic efficacy of EGFR-targeting drugs, amplification of c-Met has been identified as another acquired drug resistance mechanism.[29] c-Met modifies drug sensitivity to gefitinib through HER3-dependent activation of the PI3K/Akt pathway.[25] Moreover, Cappuzzo et al.[30] reported that gefitinib-treated patients with a high-HER3 gene copy number had significantly higher response rates and times to progression, although with no improvement in overall survival. Nuclear expression of YB-1 also affected expression of c-Met in two NSCLC cell lines in culture, but we could not observe any significant correlation between nuclear YB-1 expression and c-Met expression in NSCLC. This suggests that it is unlikely that nuclear YB-1 expression determines c-Met expression in patients with NSCLC.

Nuclear YB-1 expression is often associated with poor prognosis in various human malignancies, including breast cancer.[4–10] In NSCLC, our previous IHC study on 196 patients demonstrated that nuclear YB-1 expression is significantly associated with poor prognosis in all patients ($p = 0.0424$) and in patients with squamous cell carcinoma ($p = 0.0313$), but not in patients with adenocarcinoma ($p = 0.2015$).[8] This study demonstrated a close association of nuclear YB-1 expression with poor prognosis in all patients ($p = 0.028$) and in patients with adenocarcinoma ($p = 0.007$), but not in patients with squamous cell carcinoma ($p = 0.381$). This inconsistency may result from the small number of patients with squamous cell carcinoma in this study. The results of the Cox regression analysis given in Table 3 provide similar estimates of the HR of nuclear YB-1 expression in adenocarcinoma and squamous cell carcinoma, although they were not necessarily statistically significant. Further studies with more definitive clinicopathological characterization of the patients included are required to establish the types of NSCLC in which nuclear expression of YB-1 predicts poor prognosis.

Of patients with NSCLC ($n = 104$) tested in this study, we examined whether therapeutic efficacies of gefitinib were associated with expression levels of nuclear YB-1 expression when recurrent 26 patients (24 adenocarcinoma and two squamous cell carcinoma) were treated with gefitinib. Although the number of treated patients was small, the absence or presence of nuclear YB-1 expression shows a significant correlation with differences in the survival curves after progression disease. Concerning EGFR mutations that are highly susceptible to the therapeutic efficacy of gefitinib, we also observed statistically significant differences between patients with mutant EGFR and those with wild-type EGFR (Azuma et al, unpublished data). Nuclear YB-1 expression might have a significant predictive value for progression disease in patients with NSCLC when treated with EGFR-targeting drug. Further study is in progress whether nuclear expression of YB- 49 could be associated with gefitinib-susceptible EGFR mutations.

In conclusion, our results show that nuclear YB-1 expression is strongly associated with overall survival of patients with NSCLC ($n = 104$). Of the EGFR family proteins, nuclear YB-1 expression is associated with expression of HER2 in both histologic types of NSCLC and of HER3 in squamous cell carcinoma type of NSCLC. Therefore, expression of YB-1 in the nucleus might affect the therapeutic efficacy of EGFR-targeting drugs. Nuclear YB-1

expression is associated with progressive disease survival of patients with NSCLC (n = 26) when treated with gefitinib. Together, these observations indicate that nuclear YB-1 is a novel biomarker in NSCLC.

ACKNOWLEDGMENTS

Supported by a grant-in-aid for Scientific Research on Priority Areas, Cancer, from the Ministry of Education, Culture, Sports, Science and Technology of Japan (to M.O.), and by the 3rd Term Comprehensive Control Research for Cancer from the Ministry of Health, Labor and Welfare, Japan (to M.K.). Also supported, in part, by the Formation of Innovation Center for Fusion of Advanced Technologies, Kyushu University, Japan (to M.O., Y.B., and M.K.).

The authors thank Kimitoshi Kohno and Hiroto Izumi (University of Occupational and Environmental Health) for their fruitful discussion.

REFERENCES

1. Matsumoto K, Wolffe AP. Gene regulation by Y-box proteins: coupling control of transcription and translation. *Trends Cell Biol* 1998;8:318–323.
2. Kohno K, Izumi H, Uchiumi T, Ashizuka M, Kuwano M. The pleiotropic functions of the Y-box-binding protein, YB-1. *Bioessays* 2003;25:691–698.
3. Kuwano M, Oda Y, Izumi H, et al. The role of nuclear Y-box binding protein 1 as a global marker in drug resistance. *Mol Cancer Ther* 2004;3:1485–1492.
4. Kamura T, Yahata H, Amada S, et al. Is nuclear expression of Y-box binding protein-1 a new prognostic factor in ovarian serous adenocarcinoma? *Cancer* 1999;85:2450–2454.
5. Oda Y, Ohishi Y, Basaki Y, et al. Prognostic implication of the nuclear localization of the Y-box binding protein-1 and CXCR4 expression in ovarian cancer: their correlation with activated Akt, LRP/MVP and *P*-glycoprotein expression. *Cancer Sci* 2007;98:1020–1026.
6. Ladomery M, Sommerville J. A role for Y-box proteins in cell proliferation. *Bioessays* 1995;17:9–11.
7. Oda Y, Kohashi K, Yamamoto H, et al. Different expression profiles of Y-box-binding protein-1 and multidrug resistance-associated proteins between alveolar and embryonal rhabdomyosarcoma. *Cancer Sci* 2008;99:726–732.
8. Shibahara K, Sugio K, Osaki T, et al. Nuclear expression of the Y-box binding protein as a novel marker of disease progression in non-small cell lung cancer. *Clin Cancer Res* 2001;7:3151–3155.
9. Fujii T, Kawahara A, Basaki Y, et al. Expression of HER2 and estrogen receptor alpha depends upon nuclear localization of Y-box binding protein-1 in human breast cancers. *Cancer Res* 2008;68:1504–1512.
10. Faury D, Nantel A, Dunn SE, et al. Molecular profiling identifies prognostic subgroups of pediatric glioblastoma and shows increased YB-1 expression in tumors. *J Clin Oncol* 2007;25:1196–1208.
11. Sutherland BW, Kucab J, Wu J, et al. Akt phosphorylates the Y-box binding protein 1 at Ser 102 located in the cold shock domain and affects the anchorage-independent growth of breast cancer cells. *Oncogene* 2005;24:4281–4292.
12. Basaki Y, Hosoi F, Oda Y, et al. Akt-dependent nuclear localization of Y-box binding protein 1 in acquisition of malignant characteristics by human ovarian cancer cells. *Oncogene* 2007;26:2736–2746.
13. Jurchott K, Bergmann S, Stein U, et al. YB-1 as a cell cycle-regulated transcription factor facilitating cyclin A and B1 gene expression. *J Biol Chem* 2003;278:27988–27996.
14. Bergmann S, Royer-Pokara B, Fietze E, et al. YB-1 provokes breast cancer through the induction of chromosomal instability that emerges from mitotic failure and centrosome amplification. *Cancer Res* 2005;65:4078–4087.
15. Lu ZH, Books JT, Ley TJ. YB-1 is important for late-stage embryonic development, optimal cellular stress responses, and the prevention of premature senescence. *Mol Cell Biol* 2005;25:4625–4637.
16. Uchiumi T, Fotovati A, Sasaguri T, et al. YB-1 is important for an early stage embryonic development: neural tube formation and cell proliferation. *J Biol Chem* 2006;281:40440–40449.
17. Berquin IM, Pang B, Dziubinski ML, et al. Y-box-binding protein 1 confers EGF independence to human mammary epithelial cells. *Oncogene* 2005;24:3177–3186.
18. Wu J, Lee C, Yokom D, et al. Disruption of the Y-box binding protein-1 results in suppression of the epidermal growth factor receptor and HER-2. *Cancer Res* 2006;66:4872–4879.
19. Janz M, Harbeck N, Dettmar P, et al. Y-box factor YB-1 predicts drug resistance and patient outcome in breast cancer independent of clinically relevant tumor biologic factors HER2, uPA and PAI-1. *Int J Cancer* 2002;97:278–282.
20. Stratford AL, Habibi G, Astanehe A, et al. Epidermal growth factor receptor (EGFR) is transcriptionally induced by the Y-box binding protein-1 (YB-1) and can be inhibited with Iressa in basal-like breast cancer, providing a potential target for therapy. *Breast Cancer Res* 2007;9:R61.
21. Ohga T, Koike K, Ono M, et al. Role of the human Y box-binding protein YB-1 in cellular sensitivity to the DNA-damaging agents cisplatin, mitomycin C, and ultraviolet light. *Cancer Res* 1996;56:4224–4228.
22. Simpson EH. The interpretation of interaction in contingency table. *J R Stat Soc B* 1951;13:238–241.
23. Rothman KJ, Greenland S. (1998) Modern Epidemiology, 2nd Ed. Philadelphia: Lippincott-Raven, 1998. P. 113.
24. Hirata A, Hosoi F, Miyagawa M, et al. HER2 overexpression increases sensitivity to gefitinib, an epidermal growth factor receptor tyrosine kinase inhibitor, through inhibition of HER2/HER3 heterodimer formation in lung cancer cells. *Cancer Res* 2005;65:4253–4260.
25. Engelman JA, Jänne PA. Mechanisms of acquired resistance to epidermal growth factor receptor tyrosine kinase inhibitors in non-small cell lung cancer. *Clin Cancer Res* 2008;14:2895–2899.
26. Schaefer G, Shao L, Totpal K, Akita RW. Erlotinib directly inhibits HER2 kinase activation and downstream signaling events in intact cells lacking epidermal growth factor receptor expression. *Cancer Res* 2007;67:1228–1238.
27. Ono M, Kuwano M. Molecular mechanisms of epidermal growth factor receptor (EGFR) activation and response to gefitinib and other EGFR-targeting drugs. *Clin Cancer Res* 2006;12:7242–7251.
28. Reinmuth N, Meister M, Muley T, et al. Molecular determinants of response to RTK-targeting agents in nonsmall cell lung cancer. *Int J Cancer* 2006;119:727–734.
29. Engelman JA. The role of phosphoinositide 3-kinase pathway inhibitors in the treatment of lung cancer. *Clin Cancer Res* 2007;13:4637–4640.
30. Cappuzzo F, Toschi L, Domenichini I, et al. HER3 genomic gain and sensitivity to gefitinib in advanced non-small-cell lung cancer patients. *Br J Cancer* 2005;93:1334–1340.

N-myc Downstream Regulated Gene 1/Cap43 Suppresses Tumor Growth and Angiogenesis of Pancreatic Cancer through Attenuation of Inhibitor of κB Kinase β Expression

Fumihito Hosoi,[1,3] Hiroto Izumi,[6] Akihiko Kawahara,[3,4] Yuichi Murakami,[1] Hisafumi Kinoshita,[5] Masayoshi Kage,[3,4] Kazuto Nishio,[7] Kimitoshi Kohno,[6] Michihiko Kuwano,[2] and Mayumi Ono[1]

[1]Department of Pharmaceutical Oncology, Graduate School of Pharmaceutical Sciences and [2]Innovation Center for Medical Redox Navigation, Kyushu University, Fukuoka, Japan; [3]Research Center for Innovative Cancer Therapy, Kurume University; [4]Department of Pathology, Kurume University Hospital; [5]Department of Surgery, Kurume University School of Medicine, Kurume, Japan; [6]Department of Molecular Biology, University of Occupational and Environmental Health, Kitakyushu, Japan; and [7]Department of Genome Biology, Kinki University School of Medicine, Osaka, Japan

Abstract

N-myc downstream regulated gene 1 (NDRG1)/Cap43 expression is a predictive marker of good prognosis in patients with pancreatic cancer as we reported previously. In this study, NDRG1/Cap43 decreased the expression of various chemoattractants, including CXC chemokines for inflammatory cells, and the recruitment of macrophages and neutrophils with suppression of both angiogenesis and growth in mouse xenograft models. We further found that NDRG1/Cap43 induced nuclear factor-κB (NF-κB) signaling attenuation through marked decreases in inhibitor of κB kinase (IKK) β expression and IκBα phosphorylation. Decreased IKKβ expression in cells overexpressing NDRG1/Cap43 resulted in reduction of both nuclear translocation of p65 and p50 and their binding to the NF-κB motif. The introduction of an exogenous IKKβ gene restored NDRG1/Cap43-suppressed expression of melanoma growth-stimulating activity α/CXCL1, epithelial-derived neutrophil activating protein-78/CXCL5, interleukin-8/CXCL8 and vascular endothelial growth factor-A, accompanied by increased phosphorylation of IκBα in NDRG1/Cap43-expressing cells. In patients with pancreatic cancer, NDRG1/Cap43 expression levels were also inversely correlated with the number of infiltrating macrophages in the tumor stroma. This study suggests a novel mechanism by which NDRG1/Cap43 modulates tumor angiogenesis/growth and infiltration of macrophages/neutrophils through attenuation of NF-κB signaling. [Cancer Res 2009;69(12):4983–91]

Introduction

N-myc downstream regulated gene 1 (NDRG1)/Cap43 is one of the metastasis suppressor genes (1), and expression of NDRG1/Cap43 is regulated by oncogenes (*N-myc* and *C-myc*) and tumor suppressor genes (*p53*, *VHL*, and *PTEN*; ref. 2). Expression of NDRG1/Cap43 protein is often elevated in many types of human tumors. In human cancer, expression of NDRG1/Cap43 depends on tumor type and differentiation status (2). Consistent with this idea, NDRG1/Cap43 expression in cancer cells is a predictive marker of good prognosis in patients with neuroblastoma or cancers of the prostate, breast, esophagus, colon, and pancreas (3–10), whereas its expression is a predictive marker of poor prognosis in patients with liver and cervical cancer (11, 12).

We previously identified *NDRG1/Cap43* as one of the nine genes that are highly expressed in cancerous regions of human renal cell carcinoma (13), and its expression is closely associated with the *VHL* oncosuppressor gene (14). We further showed that expression of NDRG1/Cap43 is associated with a marked decrease of tumor angiogenesis in mice bearing human pancreatic cancer xenografts and that NDRG1/Cap43 markedly suppresses the expression of matrix metalloproteinase-9, vascular endothelial growth factor (VEGF), and interleukin (IL)-8/CXCL8. Moreover, expression of NDRG1/Cap43 has been associated with decreased microvessel density (MVD) and differentiation or depth of invasion in cancer cells in patients with pancreatic cancer (5).

In the present study, we further examined how NDRG1/Cap43 modulates tumor growth and angiogenesis in pancreatic cancer. Because microarray analysis in this study and our previous studies showed that expression of some angiogenesis- and inflammation-related factors were markedly down-regulated by NDRG1/Cap43, we hypothesized that inflammation could be somehow associated with the NDRG1/Cap43-induced suppression of tumor growth and angiogenesis. Our results indicated that down-regulation of CXC chemokines and VEGF expression by NDRG1/Cap43 was actively involved in its suppression of angiogenesis and growth in pancreatic cancer as well as infiltration of macrophages and neutrophils, and we discuss whether attenuation of nuclear factor-κB (NF-κB) signaling plays a key role in this process.

Materials and Methods

Materials and cell lines. MIApaca-2 transfectants (Mock#2, Cap#11 and Cap#14) were maintained in DMEM supplemented with 10% fetal bovine serum and G418. The anti-NDRG1/Cap43 antibody was generated as described previously (5). Other antibodies were purchased as follows: anti-β-actin antibody (Abcam); anti-NIK, anti-TAB1/2, anti-TAK1, anti-inhibitor of κB kinase (IKK) α, anti-IKKβ, anti-IKKγ, anti-p-IκBα, anti-p65, anti-p50, anti-RelB, anti-p52, and anti-ubiquitin antibodies (Cell Signaling Technology); anti-p65 and anti-p50 antibodies for supershift analysis by electromobility shift assay (EMSA; Santa Cruz Biotechnology); anti-Flag M2 antibody (Sigma); and anti-CD68 and anti-neutrophil elastase antibodies (DAKO). Human tumor necrosis factor-α (TNF-α) and MG-132 was purchased from R&D Systems and Calbiochem.

Note: Supplementary data for this article are available at Cancer Research Online (http://cancerres.aacrjournals.org/).

Requests for reprints: Mayumi Ono, Department of Pharmaceutical Oncology, Graduate School of Pharmaceutical Sciences, Kyushu University, 3-1-1 Maidashi, Higashi-ku, Fukuoka 812-8582, Japan. Phone: 81-92-642-6296; Fax: 81-92-642-6296; E-mail: mono@phar.kyushu-u.ac.jp.

doi:10.1158/0008-5472.CAN-08-4882

Plasmid constructs. To obtain full-length cDNA of human IKKβ, PCR was carried out on a SuperScript cDNA library (Invitrogen) using the following primer pairs: 5′-ATGAGCTGGTCACCTTCCCTGACAAC-3′ and 5′-TCATGAGGCCTGCTCCAGGCAGCTG-3′ (IKKβ). The PCR product was ligated into the pGEM-T easy vector (Promega), and Flag-IKKβ was ligated into the p3xFLAG-CMV10 vector (Sigma).

Oligonucleotide microarray analysis. Duplicate samples were prepared for microarray hybridization. Total RNA (2 μg) was reverse transcribed using a GeneChip 3′-Amplification Regents One Cycle cDNA Synthesis kit (Affymetrix) and labeled with Cy5 or Cy3. The labeled cRNA was applied to the oligonucleotide microarray (Human Genome U133 Plus 2.0 Array; Affymetrix), the microarray was scanned on a GeneChip Scanner3000, and the image was analyzed using GeneChip Operating Software version 1 as described previously (15).

Determination of melanoma growth-stimulating activity α/CXCL1, epithelial-derived neutrophil activating protein-78/CXCL5, IL-8/CXCL8, and VEGF-A levels by ELISA. The concentrations of IL-8/CXCL8, VEGF-A, melanoma growth-stimulating activity α (Groα)/CXCL1, and epithelial-derived neutrophil activating protein-78 (ENA-78)/CXCL5 in the homogenized supernatant of mouse xenograft tumors and conditioned medium were measured using commercially available ELISA kits (R&D Systems) in accordance with the manufacturer's instructions.

EMSA. EMSA was done as follows. Nuclear extract (6 μg) was incubated for 15 min at room temperature with a 1×10^4 counts/min ^{32}P-labeled oligonucleotide probe in binding buffer [10 mmol/L HEPES-NaOH (pH 7.9), 1 mmol/L EDTA, 50 mmol/L NaCl, 10% glycerol, 0.1 mg/mL bovine serum albumin, 0.05% NP-40, 0.005 mg/mL DTT, 0.05 mg/mL poly(deoxyinosinic-deoxycytidylic acid)] as described previously (16). The reaction mixtures were separated on a nondenaturing 4% polyacrylamide gel, and radioactivity was detected with a FLA 5000 image analyzer (Fuji Film).

Immunoprecipitations and Western blotting. The cells treated with or without MG-132 (10 μmol/L) under 2% serum condition for 8 h were lysed in lysis buffer [50 mmol/L Tris-HCl (pH 8.0), 250 mmol/L NaCl, 0.3% NP-40, 1 mmol/L EDTA, 10% glycerol, 0.1 mmol/L Na_3VO_4] supplemented with a mixture of protease inhibitors. Lysates were incubated with anti-ubiquitin antibody for 2 h at 4°C and with protein A/G agarose for additional 1 h. After all immunoprecipitates were washed three times with lysis buffer, Western blotting was done with anti-IKKβ antibody as described previously (17). The intensity of the luminescence was quantified using a CCD camera combined with an image analysis system (LAS-1000; Fuji Film).

Animals. All animal experiments were approved by the Ethics of Animal Experiments Committee at Kyushu University Graduate School of Medical Sciences. Male athymic *nu/nu* mice were purchased from Charles River Laboratories and housed in microisolator cages maintained under a 12-h light/dark cycle. Water and food were supplied *ad libitum*. Animals were observed for signs of tumor growth, activity, feeding, and pain in accordance with the guidelines of the Harvard Medical Area Standing Committee on Animals.

Immunohistochemical analysis. MIApaca-2 transfectants were injected subcutaneously into mice (1.0×10^7 cells/0.1 mL/mouse). At day 49 after transplantation of MIApaca-2 transfectants, the tumors were fixed and immunohistochemical analysis was done as described previously (5, 18). All human tissue samples were fixed and embedded in paraffin, and immunohistochemical analysis was done as described previously (5, 18). In all tissue samples, the mean value of the number of infiltrating macrophages and neutrophils and the MVD were calculated from four or five hotspots. All counts were done by three independent observers.

Statistical analysis. Data are expressed as mean ± SD. All calculations (Welch's *t* test, Student's *t* test, and Wilcoxon/Kruskal-Wallis test) were done using JMP version 5.0 (SAS Institute).

Patients and specimens. Surgically respected specimens from 37 patients with pancreatic ductal adenocarcinoma were studied. All patients underwent surgical resection between 1991 and 1998 at the Department of Surgery, Kurume University Hospital. Informed consent was obtained from all patients, and the study protocol was approved by the Ethics Committee of Kurume University.

Results

NDRG1/Cap43 down-regulates the expression of angiogenesis- and inflammation-related genes. To understand how NDRG1/Cap43 modulates tumor angiogenesis and growth in pancreatic cancer cells, we compared the expression profiles of NDRG1/Cap43 transfectant (Cap#11) and the parental low-expression counterpart (Mock#2) of MIApaca-2 cells using a high-density oligonucleotide microarray (Supplementary Table S1).

We selected eight genes predicted to be associated with adhesion, growth, and chemotaxis (Supplementary Table S2). Because our previous study showed that NDRG1/Cap43 overexpression in pancreatic cancer cells reduced the expression of angiogenesis-related factors such as VEGF-A and IL-8/CXCL8 (5), we also selected these genes, the expression of which showed a decrease of ~0.7 (Supplementary Table S2).

We confirmed the expression of NDRG1/Cap43 in two NDRG1/Cap43 transfectants (Cap#11 and Cap#14) and their mock transfectants (Mock#2) of MIApaca-2 cells (Fig. 1*A*). We compared the expression of these genes in high- and low-NDRG1/Cap43-expressing MIApaca-2 cells by quantitative real-time PCR. From the array results, we selected NCAM1, which was up-regulated by NDRG1/Cap43, as a control. The mRNA expression levels of Groα/CXCL1, ENA-78/CXCL5, IL-8/CXCL8, and VEGF-A were significantly decreased in two NDRG1/Cap43 transfectants (Cap#11 and Cap#14) in comparison with Mock#2 cells (Supplementary Fig. S1).

We used ELISA assays to compare protein levels of chemokines among pancreatic cancer cells showing low and high expression of NDRG1/Cap43 (Fig. 1*B*). We observed that Cap#11 and Cap#14 cells showed a marked decrease in the production of Groα/CXCL1 and ENA-78/CXCL5 as well as IL-8/CXCL8.

NDRG1/Cap43 suppresses the NF-κB signaling pathway in pancreatic cancer cells. Representative angiogenic factors such as IL-8/CXCL8 and VEGF-A are regulated by NF-κB (19). We investigated whether NDRG1/Cap43 expression interfered with the NF-κB signaling pathway in pancreatic cancer cells. The phosphorylation of IκBα was activated in Mock#2 cells cultured in the presence of 2% serum compared with Cap#11 and Cap#14 cells (Fig. 1*C, left*). By contrast, in the absence of serum, there appeared to be weak activation of IκBα in Mock#2 cells. However, NDRG1/Cap43 expression level was not affected with or without serum in NDRG1/Cap43 transfectants (Fig. 1*C, left*). Next, we determined the expression levels of proteins related to the NF-κB signaling pathway to examine which molecules are responsible for the difference in the phosphorylation level of IκBα between NDRG1/Cap43 and mock transfectants. Phosphorylation of IκBα is regulated by the IKK complex, which consists of two catalytic subunits, IKKα and IKKβ, and a regulatory component, IKKγ/NEMO. The expression of IKKβ was markedly reduced in Cap#11 and Cap#14 cells compared with Mock#2 cells (Fig. 1*C, middle*). There were no differences in the expression levels of other NF-κB signaling pathway-related proteins (NIK, TAB1/2, TAK1, IKKα, and IKKγ) between NDRG1/Cap43 and mock transfectants, and the expression levels of NF-κB subunits such as p65, p50, RelB, and p52 in Cap#11 and Cap#14 cells were similar to those in Mock#2 cells (Fig. 1*C, right*). Expression of IKKβ mRNA is slightly, but not significantly, decreased in NDRG1/Cap43 transfectants (Supplementary Fig. S2). In Cap#11 and Cap#14 cells, nuclear translocation of p65 was decreased by ~50% to 70% and that of p50 was decreased by ~80% compared with Mock#2, respectively (Fig. 1*D, left*). Expression of p65 and p50 showed only a slight increase in

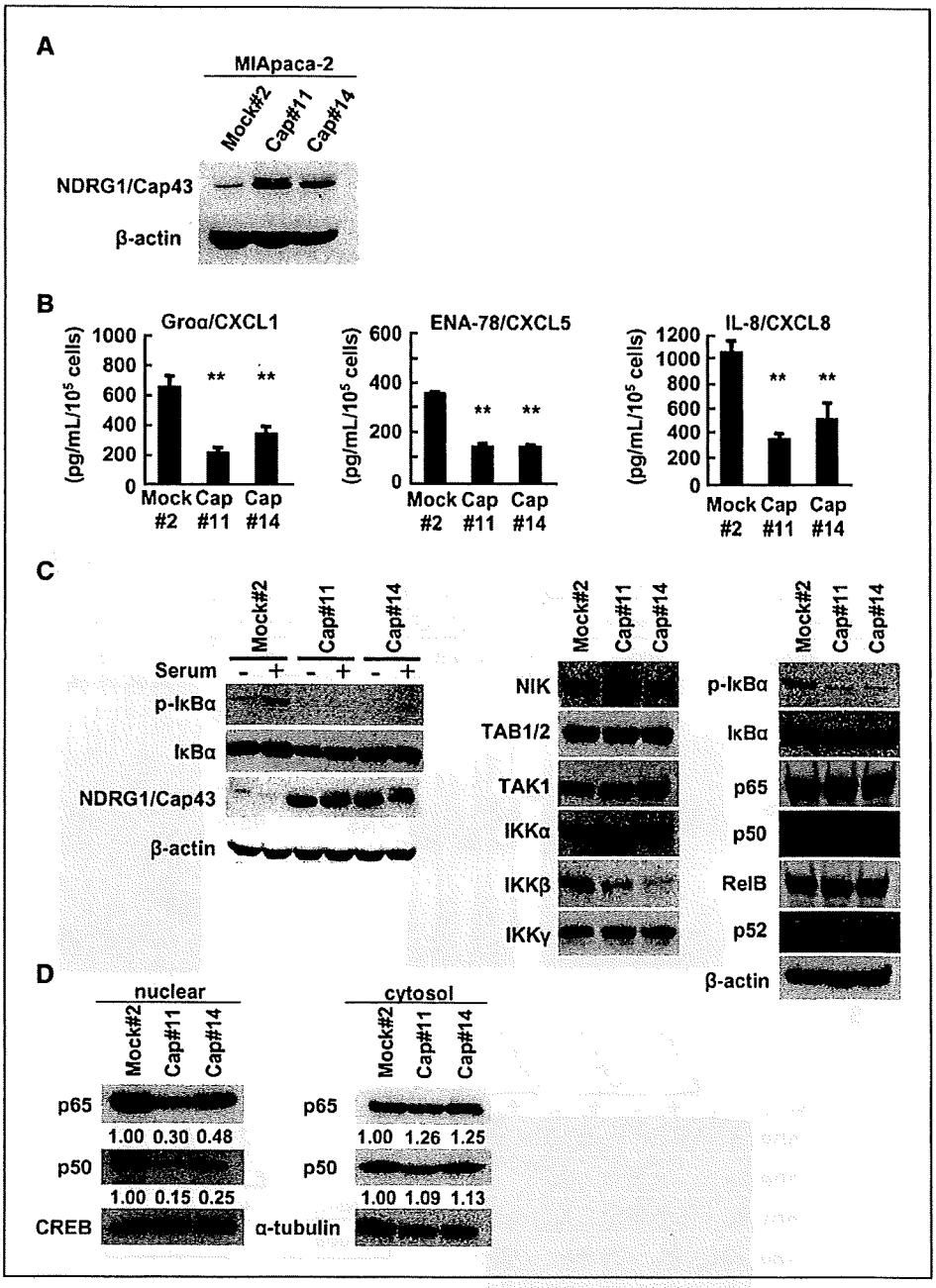

Figure 1. NDRG1/Cap43 reduces expression levels of CXC chemokines and phosphorylation of IκBα in MIApaca-2 cell lines showing low and high NDRG1/Cap43 expression. All experiments, except *A*, were done with 2% serum for 24 h. *A*, Western blot analysis of NDRG1/Cap43 expression in MIApaca-2 transfectants. *B*, ELISA assay analysis of Groα/CXCL1, ENA-78/CXCL5, and IL-8/CXCL8 protein levels in NDRG1/Cap43 and mock transfectants of MIApaca-2 cells. *Columns*, mean of three independent experiments; *bars*, SE. **, $P < 0.01$ versus Mock#2 cells. *C*, phosphorylation of IκBα and NDRG1/Cap43 expression in NDRG1/Cap43 and mock transfectants cultured with or without 2% serum for 24 h was measured by Western blotting (*left*). Western blot analysis of the expression of NF-κB signaling pathway-related proteins using whole-cell lysates prepared from NDRG1/Cap43 and mock transfectants (*middle* and *right*). *D*, Western blot analysis of the expression of p65 and p50 in nuclear (*left*) and cytosol (*right*) extracts prepared from NDRG1/Cap43 and mock transfectants. Levels of protein expression are expressed relative to the level of p65 or p50 protein in Mock#2, which is presented as 1.00.

cytosol fraction of Cap#11 and Cap#14 compared with that of Mock#2 (Fig. 1*D*, *right*).

We next performed EMSA to assess whether NDRG1/Cap43 altered the binding ability of NF-κB. One major shifted protein-DNA complex was observed after incubation of nuclear extracts prepared from Mock#2 cultured with 2% serum for 24 h (Fig. 2*A*). These complexes were specifically competed out with a 2-fold excess of the same unlabeled oligonucleotide but not with an unlabeled TRE and GC-box oligonucleotide. The protein-DNA complex after incubation of nuclear extracts was markedly decreased in Cap#11 and Cap#14 compared with Mock#2 when cultured with 2% serum. When protein-DNA complexes were incubated with antibodies against p65 and p50, supershifted bands were observed in Mock#2 (Fig. 2*A*). We next examined whether the reduced level of p-IκBα could be restored by a potent inflammatory cytokine, TNF-α, in NDRG1/Cap43 transfectants (Fig. 2*B*). TNF-α induced phosphorylation of IκBα in both Cap#11 and Cap#14 at similar levels as their parental counterpart. However, cellular levels of IKKβ in Cap#11 and Cap#14 were not affected by TNF-α. Figure 2*C* shows that TNF-α also restored the expression of IL-8/CXCL8 in Cap#11 and Cap#14 cells to levels comparable with those in Mock#2 cells. Treatment with TNF-α also enhanced the affinity of p65 and p50 for NF-κB binding sites in Cap#11 and Cap#14 at similar levels to those in their parental counterparts (Fig. 2*D*). Taken together, NDRG1/Cap43 was not involved in TNF-α-induced NF-κB signaling pathway.

IKKβ overexpression overcomes NDRG1/Cap43-induced suppression of IκBα phosphorylation and chemokine expression. Expression of IKKβ was decreased in two NDRG1/Cap43 transfectants (Cap#11 and Cap#14). We examined whether exogenous IKKβ expression was able to restore the IκBα phosphorylation in NDRG1/Cap43 transfectants. Expression of IKKβ was augmented in both NDRG1/Cap43 and mock transfectants after transfection of the exogenous IKKβ gene (Fig. 3*A*). The phosphorylation of IκBα was increased in Cap#11 to a level comparable with that in Mock#2. Expression of Groα/CXCL1, ENA-78/CXCL5, and IL-8/CXCL8 was also significantly increased after transfection of IKKβ in Cap#11 cells when there was no apparent difference in the expression levels of these chemokines between empty and IKKβ transfection in Mock#2 (Fig. 3*B*). Expression of VEGF-A was also increased in IKKβ-transfected Cap#11 cells compared with that in empty-transfected Cap#11 cells. We observed that VEFG-A expression was decreased in IKKβ-transfected Mock#2 compared with empty-transfected Mock#2 cells, but the reason for this remains unclear.

IKKβ has been reported to hold a putative ubiquitin-like domain (20). We examined whether the reduced expression of IKKβ protein was restored by proteasome inhibitor, MG-132, in Cap#11 cells. MG-132 inhibited degradation of p-IκBα in both Mock#2 and Cap#11 cells (Fig. 3*C*). Furthermore, expression of IKKβ in Cap#11 cells was restored to similar levels as in Mock#2 cells when treated with MG-132. MG-132 did not significantly affect IKKβ mRNA expression in Mock#2 ($P = 0.65$) and Cap#11 ($P = 0.48$) cells

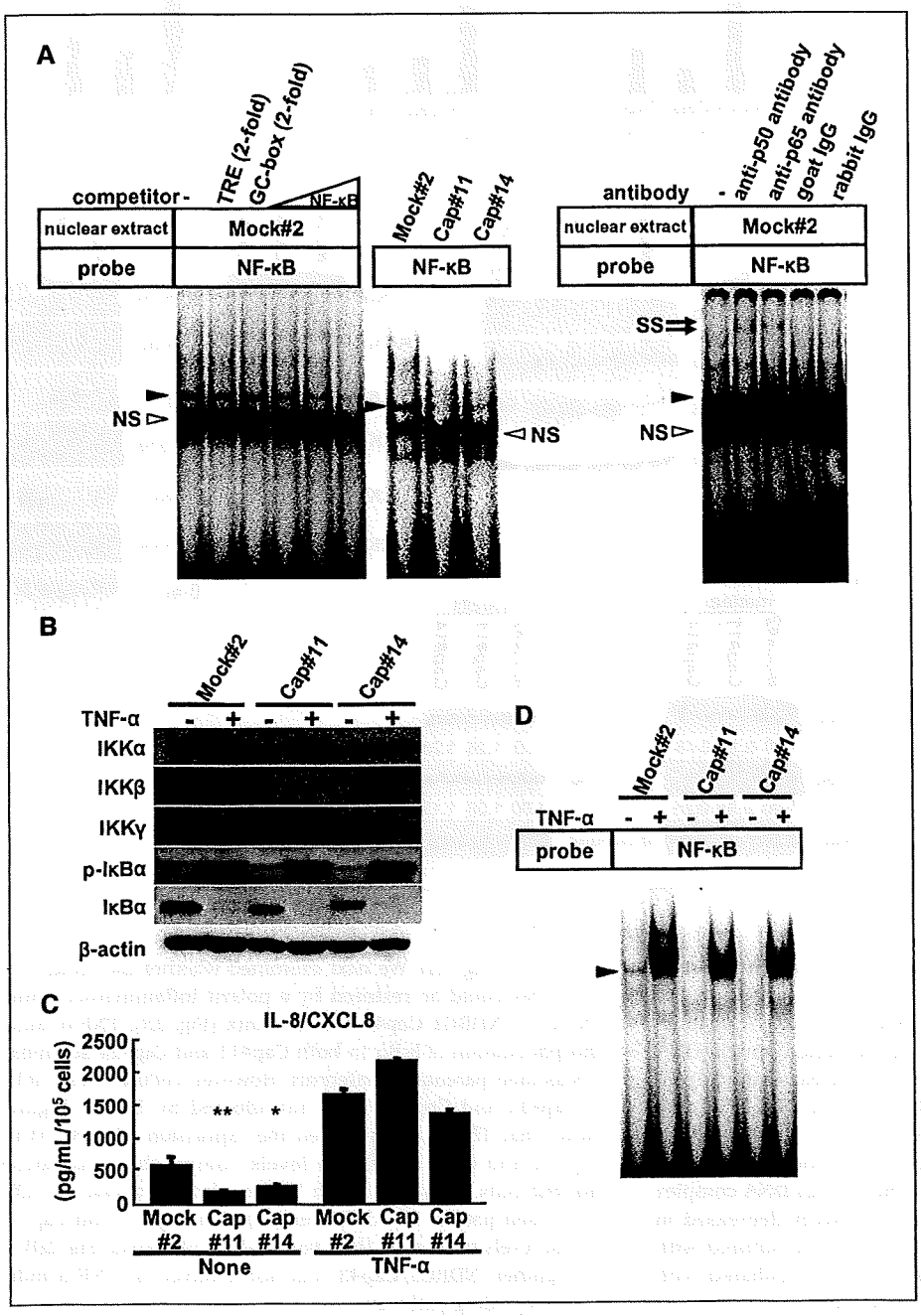

Figure 2. Suppression of binding activity of NF-κB by NDRG1/Cap43. *A*, EMSA using the NF-κB binding oligonucleotide. Nuclear extracts from three transfectants cultured in the presence of 2% serum were incubated with oligonucleotide as described in Materials and Methods. *Black arrowheads*, shifted bands; 0.08-, 0.4-, or 2-fold molar excess of unlabeled oligonucleotide was used as the competitor. A 2-fold molar excess of unlabeled oligonucleotide (TRE and GC-box) was used as a negative control for this competition assay. *Arrows*, positions of the supershifted bands (*SS*); *NS*, nonspecific band (*white arrowheads*). *B*, Western blot analysis of IκBα phosphorylation and expression of IKKα, IKKβ, and IKKγ in NDRG1/Cap43 and mock transfectants under serum-free conditions with or without TNF-α (20 ng/mL) stimulation for 30 min. *C*, ELISA assay analysis of IL-8/CXCL8 protein levels in NDRG1/Cap43 and mock transfectants of MIApaca-2 cells under serum-free conditions with or without TNF-α (20 ng/mL) for 24 h. *Columns*, mean of three independent experiments; *bars*, SE. *, $P < 0.05$; **, $P < 0.01$ versus mock transfectants. *D*, EMSA using the NF-κB binding oligonucleotide with nuclear extracts from three transfectants under serum-free conditions with or without TNF-α (20 ng/mL) for 30 min. *Black arrowheads*, shifted bands.